Journal of Cosmology and Astroparticle Physics

SISSA

Gravitational wave background from vacuum and thermal fluctuations during axion-like inflation

Journal of Cosmology and Astroparticle Physics
An IOP and SISSA journal

Gravitational wave background from vacuum and thermal fluctuations during axion-like inflation

P. Klose, M. Laine and S. Procacci

AEC, Institute for Theoretical Physics, University of Bern,
Sidlerstrasse 5, CH-3012 Bern, Switzerland

E-mail: pklose@itp.unibe.ch, laine@itp.unibe.ch, procacci@itp.unibe.ch

Received October 28, 2022
Revised November 7, 2022
Accepted November 22, 2022
Published December 13, 2022

Abstract. We revisit the framework of axion-like inflation in view of the possibility that the coupling of the inflaton to a non-Abelian topological charge density could lead to the generation of a rapidly thermalizing heat bath. Both dispersive (mass) and absorptive (friction) effects are included. For phenomenologically viable parameters, the system remains in a weak regime of warm inflation (thermal friction $\ll$ Hubble rate). For tensor perturbations we derive an interpolating formula that incorporates both vacuum and thermal production. The latter yields a model-independent frequency shape $\sim f_0^3$ in the LISA window, whose coefficient allows to measure the maximal shear viscosity of the thermal epoch. It is a challenge, however, to find models where the coefficient is large enough to be observable.

Keywords: particle physics - cosmology connection, primordial gravitational waves (theory), inflation, axions

ArXiv ePrint: 2210.11710

https://doi.org/10.1088/1475-7516/2022/12/020

JCAP12(2022)020

Contents

JCAP12(2022)020

1 Introduction

In order to make maximal use of the upcoming LISA gravitational wave interferometer, it is important to have frequency templates for various phenomena that might take place in the early universe. Among the most important sources of gravitational waves is inflation [1]. The corresponding energy density is constrained by the indirect effect of the gravitational background on CMB photons, parametrized by the tensor-to-scalar ratio r, which is bounded from above at small frequencies ($f_0 \ll 10^{-15}\,\mathrm{Hz}$ today[1]). It is possible that physics at a late stage of inflation leads to an additional contribution [3–6], which could increase with frequency. The LISA sensitivity peaks at $f_0 \sim (10^{-4}\text{–}10^{-1})\,\mathrm{Hz}$ [7], and ideally we could envisage a mechanism that sources an observable spectrum in this domain.

One example of such a mechanism is axion inflation [8–10]. In this case, it has been argued that an efficient tachyonic instability could convert a significant fraction of the initial energy density into gravitational radiation [11–13] (cf., e.g., ref. [14] for an overview). Therefore this is one of the models for which LISA sensitivity studies have been carried out [15].

[1]The scales probed by the CMB are normally expressed via the wave number, $p_0 \in (10^{-4}\text{–}10^{-1})\,\mathrm{Mpc}^{-1}$ [2].

It could be asked, however, how robust this scenario is. Notably, many studies concern the case of an axion coupling to Abelian gauge fields. The large signal originates when their conversion into gravitational waves proceeds without any backreaction. But backreaction must exist, even just from energy conservation (cf., e.g., refs. [16, 17] and references therein), and quite concretely if the Abelian fields are coupled to fermions [18].

If the gauge sector is non-Abelian, which appears natural from the particle physics point of view, backreaction is more substantial, as it takes place even without fermions. Such a system has been argued to interact strongly enough to thermalize already during inflation [19].[2] Thermalization maximizes backreaction, by eliminating memory of initial conditions. In this case, the fraction of energy density converted to gravitational radiation is not of order unity, but it is rather suppressed by couplings [22]. It appears interesting to estimate whether an observable signal could originate nevertheless.

Our goal is to study gravitational wave production in the case of a thermalized non-Abelian gauge sector. Previously, we have done this for the signal originating at reheating [22], which peaks at high frequencies, $f_0 \sim 10^{11}\,\mathrm{Hz}$, and can be constrained by the observable $N_{\rm eff}$.[3] Now we turn to gravitational wave production during the inflationary stage itself, with particular focus on the LISA frequency window, $f_0 \sim (10^{-4}\text{–}10^{-1})\,\mathrm{Hz}$.

To be specific, we consider a theory defined in local Minkowskian coordinates by the Lagrangian

$$\mathcal{L} \supset \frac{1}{2}\partial^\mu\varphi\,\partial_\mu\varphi - V_0(\varphi) - \frac{\varphi\,\chi}{f_a}\,, \quad \chi \equiv c_\chi\,\epsilon^{\mu\nu\rho\sigma}g^2F^c_{\mu\nu}F^c_{\rho\sigma}\,, \quad c_\chi \equiv \frac{1}{64\pi^2}\,, \tag{1.1}$$

where φ is the inflaton field, $F^c_{\mu\nu} \equiv \partial_\mu A^c_\nu - \partial_\nu A^c_\mu + g f^{cde} A^d_\mu A^e_\nu$ is the Yang-Mills field strength, $N_{\rm c}$ is the number of colours, $c \in \{1,\ldots,d_{\rm A}\}$, $d_{\rm A} \equiv N_{\rm c}^2 - 1$, $g^2 \equiv 4\pi\alpha$, and f_a is the axion decay constant. We stress that our φ is not a physical QCD or dark matter axion, but a more general field, heavier than would-be dark matter candidates, and unstable.

The potential $V_0(\varphi)$ appearing in eq. (1.1) requires some elaboration. We consider $V_0(\varphi)$ to be a "bare" vacuum potential, whereas $V(\varphi)$ denotes a potential including dynamical effects from gauge field interactions (including thermal effects if the system has thermalized). Omitting thermal effects for the moment (these are added in section 2.3) and postponing variations of the potential till later on (cf. section 4.3), we carry out our baseline discussion with the ansatz

$$V(\varphi) \simeq m^2 f_b^2 \left[1 - \cos\left(\frac{\varphi}{f_b}\right)\right]. \tag{1.2}$$

In eq. (1.2), $\sqrt{m f_b} \sim \Lambda_{\rm UV}$ corresponds to the confinement scale of some unified theory. Technically, we assume that inflationary physics has an energy scale $\epsilon_\varphi \ll \Lambda_{\rm UV}$, but that ϵ_φ is much larger than the confinement scale $\Lambda_{\rm IR}$ of some unbroken SU($N_{\rm c}$) subgroup, whose coupling $\alpha \ll 1$ is weak. It is the latter gauge group that has been displayed in eq. (1.1).

On the semiclassical level, the periodicity of eq. (1.2) is related to the topological character of χ in eq. (1.1), i.e. that χ evaluates to an integer for smooth vacuum configurations. This implies that $f_b = f_a$, and we assume this relation throughout. Given the operator in eq. (1.1), radiative corrections to $V(\varphi)$ are suppressed by powers of $1/f_a^2$, and appear on par with effects

[2] The obstacles for warm inflation raised in ref. [20] are evaded in the case of non-Abelian axion inflation, as reviewed in the introduction of ref. [21].

[3] This parametrizes the overall energy density throuh the effective number of relativistic "neutrino-like" species, so that a non-zero $N_{\rm eff} - 3$ originates either from non-trivial Standard Model dynamics, or from beyond the Standard Model degrees of freedom.

JCAP12(2022)020

from higher-dimensional operators that have been omitted from eq. (1.1). However, infrared (IR) contributions, such as thermal corrections, can be consistently included at $\mathcal{O}(1/f_a^2)$.

This paper is organized as follows. We start by considering the semiclassical evolution of the average inflaton field, including thermal friction and mass corrections (cf. section 2). Then we discuss how this background sources tensor perturbations, or gravitational waves (cf. section 3). After analyzing the shape of the corresponding spectrum (cf. section 4), conclusions can be offered (cf. section 5). Appendix A elaborates on "dispersive" relations between thermal friction and mass effects, implying that both should be considered on equal footing.

2 Background solution

Assuming that the gauge fields appearing in eq. (1.1) thermalize rapidly, they form a radiation bath to which the inflaton couples. As a first step, we recall the resulting evolution equations, yielding what is called the background solution. This topic agrees technically with the setup of warm inflation [23, 24], recently studied with renewed interest in the axion inflation context [21, 25–30]. However, thermal mass corrections (cf. section 2.3) have often been omitted, so we devote particular attention to this aspect.

Before proceeding, it is important to note that the corrections originating from the gauge field heat bath depend not only on the temperature, but also on the curvature of the space in which the gauge fields live, which is parametrized by the Hubble rate $H \equiv \dot{a}/a$, where a is the scale factor in Friedmann-Robertson-Walker coordinates. Thermal effects can be consistently included if the thermal scattering or equilibration rate, $\sim \alpha^2 T$, is large compared with the Hubble rate, $\alpha^2 T \gtrsim H$. In this regime, corrections proportional to the Hubble rate are small compared with the thermal ones, $H^2 \ll T^2$. The computations are carried out in a local Minkowskian frame, and subsequently the equivalence principle is invoked in order to convert the results to a general frame. If the dynamical solution leads to a smaller temperature, then the assumption of a thermal medium is not self-consistent. But in this regime thermal corrections are very small, so their incomplete inclusion entails only an insignificant error.

2.1 Equations of motion

To get the background solution, we consider a homogeneous average field, $\varphi(t, \mathbf{x}) \to \bar{\varphi}(t)$, and couple the inflaton to the energy-momentum tensor of a plasma. Simultaneously we include thermal corrections (whose form is specified in section 2.3) in the effective potential from eq. (1.2). Then the classical equations of motion reduce to

$$\ddot{\bar{\varphi}} + (3H + \Upsilon)\dot{\bar{\varphi}} + V_\varphi \simeq 0 \,, \tag{2.1}$$

$$\dot{e}_r + 3H(e_r + p_r - TV_{,T}) - T\dot{V}_{,T} \simeq \Upsilon \dot{\bar{\varphi}}^2 \,, \tag{2.2}$$

where $V_{,x} \equiv \partial_x V$. The form of these equation ensures overall energy conservation, with a gradual transfer of energy from $\bar{\varphi}$ to radiation.[4] The Friedmann equation closes the system,

$$H = \frac{\dot{a}}{a} = \sqrt{\frac{8\pi}{3}} \frac{\sqrt{e_r + V - TV_{,T} + \dot{\bar{\varphi}}^2/2}}{m_{\rm pl}} \,, \tag{2.3}$$

where we have parametrized the Newton constant as $G \equiv 1/m_{\rm pl}^2$, $m_{\rm pl} = 1.22091 \times 10^{19}\,\text{GeV}$.

[4] The opposite process, stochastic transfer of energy from the plasma to φ, can be included through a noise term in eq. (2.1) [31]. This is important for the origin of scalar perturbations, but plays no practical role for the background solution, or for the tensor perturbations discussed in section 3.

JCAP12(2022)020

As for e_r and p_r, we note that at temperatures below the confinement scale of the SU(N_c) group in eq. (1.1) ($T \ll \Lambda_{\rm IR}$), the heat capacity is exponentially small. Then, a small release of entropy leads to a large change in the temperature. Therefore, we may assume that the system has already heated up to a temperature above $\Lambda_{\rm IR}$ (which should be minuscule compared with the Planck scale, or the ultraviolet confinement scale $\Lambda_{\rm UV}$ mentioned below eq. (1.2)). This simplifies matters, as we may use a conformal equation of state for radiation, $p_r \simeq g_*\pi^2 T^4/90$. For $T \gg \Lambda_{\rm IR}$, we can assume $\alpha \ll 1$, which is beneficial for our analysis (cf. the discussion below eq. (2.15)).

Apart from the evolution of the inflaton and the temperature, dictated by eqs. (2.1) and (2.2), we also solve for the increase of the number of e-folds, $N \equiv \ln(a/a_{\rm ref})$, from

$$\dot{N} = H \,. \tag{2.4}$$

Here $a_{\rm ref}$ denotes the scale parameter at some initial time, $t = t_{\rm ref}$, specified for the numerics later on (cf. caption of figure 3). Furthermore it is important to know how the ratio of a comoving momentum to the Hubble rate, $k/(aH)$, changes with time. This can be expressed as

$$\frac{k}{(aH)(t)} = \frac{k\, e^{-N(t)}}{a_{\rm ref}\, H(t)} \,. \tag{2.5}$$

As long as $H \approx$ constant, this ratio decreases exponentially. Once inflation ends, H starts to decrease and N is almost constant, whence the ratio increases (cf. figure 3). The factor $a_{\rm ref}$ drops out later on, when physical results are expressed in terms of present-day observables.

As a technical remark, we note that if we integrate over a long period of time, interpolating between the inflationary and the radiation epochs, then it is favourable to replace t by another variable in eqs. (2.1) and (2.2). For this purpose, we employ in section 4

$$x - x_{\rm ref} \;\equiv\; \ln\!\left(\frac{t}{t_{\rm ref}}\right) . \tag{2.6}$$

2.2 Thermal friction coefficient

A key role in eqs. (2.1) and (2.2) is played by the friction coefficient, Υ. It needs to be fixed as it originates from the operator in eq. (1.1), which couples the inflaton to the heat bath. The value is determined by the response function of the medium evaluated at the appropriate frequency scale [21], thereby incorporating both vacuum physics (for $\omega \sim m \gg \pi T$) and thermal physics. The latter is important particularly at high temperatures, if we are driven to the regime $\omega \lesssim m \lesssim \alpha N_c T$.

It was indicated above that the frequency scale ω was chosen to coincide with the mass scale at the minimum of the potential, m. As an alternative, we have also tested a dynamically evolving ω, defined as $\omega_{\rm dyn} \equiv \sqrt{\max(0, V_{\varphi\varphi})}$. Even if this does have an effect, influencing the results quantitatively on the $\mathcal{O}(1)$ level, we have not found any qualitative changes, and therefore stick to the simpler choice $\omega = m$ in the following.

It has been appreciated in refs. [21, 25–30] that determining the value of Υ in the regime $\omega \lesssim \alpha N_c T$ requires non-perturbative input. Indeed the value at $\omega \to 0$ can be taken over from older lattice simulations [32], while the broader shape, extending to $\omega \sim \alpha N_c T$, has only been measured recently [33]. Larger frequencies can be addressed with a perturbative

JCAP12(2022)020

computation [34], and subsequently the parts can be put together,

$$\Upsilon \simeq \frac{d_{\rm A}\alpha^2}{f_a^2}\left\{\kappa\,(\alpha N_{\rm c}T)^3\,\frac{1+\frac{\omega^2}{(c_{\rm IR}\alpha^2N_{\rm c}^2T)^2}}{1+\frac{\omega^2}{(c_{\rm M}\alpha N_{\rm c}T)^2}}+\Big[1+2n_{\rm B}\Big(\frac{\omega}{2}\Big)\Big]\frac{\pi\omega^3}{(4\pi)^4}\right\}, \tag{2.7}$$

$$\kappa\simeq 1.5\,,\quad c_{\rm IR}\simeq 106\,,\quad c_{\rm M}\simeq 5.1\,, \tag{2.8}$$

where $n_{\rm B}(x)\equiv 1/(e^{x/T}-1)$ is the Bose distribution. We fix $N_{\rm c}=3$ for numerical illustrations and approximate the coupling according to eq. (2.17).

2.3 Thermal mass correction

The potential V in eqs. (2.1)–(2.3) can be partly parametrized by its curvature around the global minimum, which we call the mass squared. The full shape contains other parameters as well, and their treatment is not as easy to handle in a universal manner; further comments on this follow below eq. (2.15). The mass squared experiences thermal corrections, which can formally be related to the real part of the same retarded correlator, $C_{\rm R}$, whose imaginary part determines Υ [21]. In appendix A we summarize general issues associated with the relation of the real and imaginary parts of $C_{\rm R}$, whereas in the remainder of the present section, we show how $\mathrm{Re}\,C_{\rm R}$ can be determined through a perturbative computation.

A compact expression for $C_{\rm R}$ can be given within the imaginary-time formalism of thermal field theory. From eq. (3.2) of ref. [35], after inverting the overall sign to conform with Minkowskian conventions, we have

$$C_{\rm R}(\omega+i0^+)=8d_{\rm A}c_\chi^2(D-3)(D-2)g^4\oint\!\!\!\!\!\!\sum_{\!\!Q}\left\{\frac{K^4}{Q^2(Q-K)^2}-\frac{2K^2}{Q^2}\right\}_{K\to(-i[\omega+i0^+],\mathbf{0})}+\mathcal{O}(g^6)\,, \tag{2.9}$$

where $D\equiv 4-2\epsilon$ is the dimension of spacetime and $\oint\!\!\!\!\!\!\sum_{\!\!Q}$ denotes a bosonic Matsubara sum-integral. After carrying out the Matsubara sum, the result contains terms with and without the Bose distribution, $n_{\rm B}$. The terms without $n_{\rm B}$ are vacuum contributions, and can be determined analytically, leading to an UV divergent result, which requires renormalization. The terms with Bose distributions are finite, but need to be evaluated numerically.

We obtain, with $\bar\mu^2\equiv 4\pi\mu^2e^{-\gamma_{\rm E}}$ denoting the $\overline{\rm MS}$ renormalization scale,

$$\mathrm{Re}\,C_{\rm R}(\omega)=\frac{d_{\rm A}c_\chi^2g^4\omega^2}{\pi^2f_a^2}\left\{\omega^2\mu^{-2\epsilon}\left(\frac{1}{\epsilon}+\ln\frac{\bar\mu^2}{\omega^2}-1\right)+\int_0^\infty\mathrm{d}q\,\mathbb{P}\left[\frac{16q^3n_{\rm B}(q)}{(q-\frac{\omega}{2})(q+\frac{\omega}{2})}\right]\right\}, \tag{2.10}$$

where $\mathbb{P}$ denotes the principal value. The vacuum part agrees with eq. (5.2) of ref. [21]. The thermal part has the limiting values $\mathrm{Re}\,C_{\rm R}(\omega)|_T\overset{T\ll\omega}{\to}-64d_{\rm A}c_\chi^2g^4\pi^2T^4/(15f_a^2)$ and $\mathrm{Re}\,C_{\rm R}(\omega)|_T\overset{T\gg\omega}{\to}8d_{\rm A}c_\chi^2g^4\omega^2T^2/(3f_a^2)$, and it crosses zero at $\omega\approx 5.2T$.

The effective mass squared is given by [21]

$$m_T^2\approx m^2-\mathrm{Re}\,C_{\rm R}(m)\,. \tag{2.11}$$

The effective theory description is self-consistent provided that $\mathrm{Re}\,C_{\rm R}(m)\ll m^2$. While this is certainly true for $T\ll m$, the constraint becomes non-trivial for $T\gg m$, where $\mathrm{Re}\,C_{\rm R}(m)>0$. Inserting the limiting value from below eq. (2.10), m_T^2 remains positive for $\alpha^2T^2\ll f_a^2$, which is just the condition for the validity of the effective theory.

JCAP12(2022)020

For eqs. (2.2) and (2.3), we need the first and second temperature derivatives of the effective mass squared,

$$\partial_T m_T^2 = -\frac{16 d_{\rm A} c_\chi^2 g^4 m^2}{\pi^2 f_a^2 T^2} \int_0^\infty {\rm d}q\, \mathbb{P} \left\{ \frac{q^4 n_{\rm B}(q)[1+n_{\rm B}(q)]}{(q-\frac{m}{2})(q+\frac{m}{2})} \right\} , \tag{2.12}$$

$$\partial_T^2 m_T^2 = -\frac{16 d_{\rm A} c_\chi^2 g^4 m^2}{\pi^2 f_a^2 T^3} \int_0^\infty {\rm d}q\, \mathbb{P} \left\{ \frac{q^5 n_{\rm B}(q)[1+n_{\rm B}(q)]}{(q-\frac{m}{2})(q+\frac{m}{2})} \left[\frac{1+2n_{\rm B}(q)}{T} - \frac{2}{q} \right] \right\} . \tag{2.13}$$

Given the asymptotic values mentioned below eq. (2.10), both are positive for $T \ll m$ and negative for $T \gg m$; they again cross zero at $m \sim 2\pi T$. The physical quantities in which eqs. (2.12) and (2.13) appear, are the entropy density and the heat capacity, respectively,

$$\bar{s} = s_r - V_T \simeq \frac{2g_*\pi^2 T^3}{45} - \partial_T m_T^2\, f_b^2 \left[1 - \cos\left(\frac{\bar{\varphi}}{f_b} \right) \right] , \tag{2.14}$$

$$\bar{c} = c_r - T V_{TT} \simeq \frac{2g_*\pi^2 T^3}{15} - T\partial_T^2 m_T^2\, f_b^2 \left[1 - \cos\left(\frac{\bar{\varphi}}{f_b} \right) \right] . \tag{2.15}$$

For the second steps in eqs. (2.14) and (2.15), we have assumed that the functional form of eq. (1.2) remains intact in the thermal corrections, i.e. that the parameter f_b^2 does not get corrected. The logic here is that its inverse $1/f_b^2$ represents the expansion parameter of the effective theory treatment, and that corrections to it would only arise at order $1/f_b^4$. However, other philosophies could be envisaged, for instance that we subtract from V the vacuum quadratic part and only apply the thermal correction to this one,

$$V^{\rm alt} \simeq m^2 f_b^2 \left[1 - \cos\left(\frac{\bar{\varphi}}{f_b} \right) \right] + \frac{m_T^2 - m^2}{2} \bar{\varphi}^2 . \tag{2.16}$$

The corresponding $\bar{s}$ and $\bar{c}$ are like in eqs. (2.14) and (2.15), but with $1-\cos(\bar{\varphi}/f_b)$ expanded to quadratic order in $\bar{\varphi}$. We have checked that our numerical results in section 4 remain unaltered if we replace V by $V^{\rm alt}$.

For a consistent treatment, both eq. (2.14) and (2.15) should remain positive. The tricky domain is that of low temperatures, where eqs. (2.12) and (2.13) are positive. Recalling the asymptotics from below eq. (2.10) and the minus sign from eq. (2.11), and setting $f_a = f_b$, we see that the relative corrections are small provided that $\alpha^2 \ll 1$. This assumption we are making in any case, as we are employing a non-interacting form for the radiation contributions s_r and c_r to $\bar{s}$ and $\bar{c}$, respectively (cf. the discussion in section 2.1).

For the practical computations, we need to insert a value for the gauge coupling. Following ref. [21], eq. (2.10) is renormalized in the $\overline{\rm MS}$ scheme, setting $\bar{\mu} \to f_a (= f_b)$, whereas the coupling is approximated as

$$g^2 \simeq \frac{3(4\pi)^2}{22 N_{\rm c}} \ln^{-1}\left[\frac{\sqrt{(2\pi\Lambda_{\rm IR})^2 + (2\pi T)^2 + m^2}}{\Lambda_{\rm IR}} \right] . \tag{2.17}$$

The initial temperature is taken from the domain $T \gg \Lambda_{\rm IR}$, guaranteeing that $\alpha \ll 1$ (we have set $\Lambda_{\rm IR} \equiv 0.2\,{\rm GeV}$). We remark that the effective T-dependence of g^2 is formally a higher-order effect, of $\mathcal{O}(g^4)$, and therefore omitted in eqs. (2.12) and (2.13).

JCAP12(2022)020

3 Tensor perturbations

Having determined the background solution in section 2, we now turn to perturbations. While the treatment of scalar perturbations is well established, that of tensor perturbations is slightly less so, so we go through a detailed exposition.

3.1 Vacuum fluctuations in de Sitter spacetime

We start by reviewing the fluctuation spectrum of a massless[5] scalar field in de Sitter spacetime, as it turns out that tensor perturbations can be taken over from this result with minor modifications (cf. section 3.1.3). First the standard derivation is repeated in a minimal manner (cf. section 3.1.1), and subsequently we carry it out with the so-called stochastic formalism [36] (cf. section 3.1.2), as this helps to incorporate thermal fluctuations (cf. sections 3.2 and 3.3).

3.1.1 Canonical derivation

Considering a massless scalar field h, we first need to fix its normalization. Canonical normalization is specified by giving the action or the Hamiltonian in a local Minkowskian frame,

$$\mathcal{S}_{M} = -\int_{\mathcal{Y}} \frac{1}{2}\, h^{,\mu}\, h_{,\mu}\,, \quad H_{M} = \int \mathrm{d}^{3}\mathbf{y}\, \frac{1}{2}\big[\,\dot{h}^{2} + (\nabla h)^{2}\,\big]\,, \tag{3.1}$$

where $\mathcal{Y} \equiv (t, \mathbf{y})$, and we have adopted the "mostly plus" metric convention. The quantized on-shell field operator is

$$\big[\,h\,\big]_{M} = \int \frac{\mathrm{d}^{3}\mathbf{p}}{\sqrt{(2\pi)^{3} 2p}} \Big[\, a_{\mathbf{p}}\, e^{-ipt+i\mathbf{p}\cdot\mathbf{y}} + a^{\dagger}_{\mathbf{p}}\, e^{ipt-i\mathbf{p}\cdot\mathbf{y}} \Big]_{M}\,, \tag{3.2}$$

where the annihilation and creation operators $a_{\mathbf{p}}$ and $a^{\dagger}_{\mathbf{p}}$ satisfy the commutator in eq. (3.3), and $[\,]_{M}$ is a reminder of the momenta being Minkowskian.

For future reference, let us express the field operator in eq. (3.2) in co-moving conformal coordinates. We denote co-moving momenta by $\mathbf{k}$ and $\mathbf{l}$, their relations to physical momenta being $\mathbf{p} = \mathbf{k}/a$ and $\mathbf{q} = \mathbf{l}/a$. The co-moving coordinate $\mathbf{x}$ corresponds to the physical $\mathbf{y} = a\mathbf{x}$, whereas the conformal and physical times are related by $\mathrm{d}\tau = \mathrm{d}t/a$. The canonical commutator becomes

$$\big[\, a_{\mathbf{p}}, a^{\dagger}_{\mathbf{q}} \,\big] = \delta^{(3)}(\mathbf{p}-\mathbf{q}) = a^{3}\, \delta^{(3)}(\mathbf{k}-\mathbf{l}) \equiv a^{3}\, \big[\, w_{\mathbf{k}}, w^{\dagger}_{\mathbf{l}} \,\big]\,. \tag{3.3}$$

Implementing the coordinate transformation yields what will later on be interpreted as the field operator in the distant past, namely

$$\big[\,h\,\big]_{M} = \frac{1}{a} \int \frac{\mathrm{d}^{3}\mathbf{k}}{\sqrt{(2\pi)^{3} 2k}} \Big[\, w_{\mathbf{k}}\, e^{-ik\tau+i\mathbf{k}\cdot\mathbf{x}} + w^{\dagger}_{\mathbf{k}}\, e^{ik\tau-i\mathbf{k}\cdot\mathbf{x}} \Big]\,. \tag{3.4}$$

We now go to de Sitter spacetime,[6] with the scale factor $a(t) = a(t_{\mathrm{ref}})\, e^{H(t-t_{\mathrm{ref}})}$. Denoting $a' \equiv \mathrm{d}a/\mathrm{d}\tau$ and $\dot{a} \equiv \mathrm{d}a/\mathrm{d}t$, the scale factor satisfies

$$a' = \dot{a}\, \frac{\mathrm{d}t}{\mathrm{d}\tau} = H a^{2}\,. \tag{3.5}$$

[5] We are implicitly assuming that there is a (gauge) symmetry which protects the field from receiving mass corrections, as this is the case that can be applied to tensor perturbations.

[6] It is straightforward to generalize the computation to first order in slow-roll parameters [37], keeping track of a non-zero value of $\dot{H}/H^{2}$, however then the mode equations are solved by Bessel functions. As their properties are intransparent and the conclusions remain unchanged, we stick to pure de Sitter spacetime here.

JCAP12(2022)020

Choosing the range of τ as $(-\infty, 0)$ and denoting $\mathcal{H} \equiv a'/a$, this leads to

$$a = -\frac{1}{H\tau} \,, \quad \mathcal{H} = -\frac{1}{\tau} \,. \tag{3.6}$$

The massless field equation in de Sitter spacetime reads

$$h'' + 2\mathcal{H}h' - \nabla^2 h = 0 \,. \tag{3.7}$$

We stress that, contrary to a proper inflationary analysis of scalar perturbations, there is no metric perturbation here to which h couples. Going over to co-moving momentum space, with

$$h = \int \frac{\mathrm{d}^3\mathbf{k}}{(2\pi)^{3/2}} \left[w_{\mathbf{k}}\, h_k(\tau) e^{i\mathbf{k}\cdot\mathbf{x}} + w^\dagger_{\mathbf{k}}\, h^*_k(\tau) e^{-i\mathbf{k}\cdot\mathbf{x}} \right] , \tag{3.8}$$

and inserting $\mathcal{H}$ from eq. (3.6), the mode function h_k must fulfil

$$\left(\partial_\tau^2 - \frac{2}{\tau}\,\partial_\tau + k^2 \right) h_k = 0 \,. \tag{3.9}$$

This is readily solved, with the two independent solutions having the forms

$$h_k \subset \left\{ C\,(1 + ik\tau)\, e^{-ik\tau} \,, \quad C^*(1 - ik\tau)\, e^{ik\tau} \right\} . \tag{3.10}$$

The constant C is fixed so as to reproduce eq. (3.4) at $\tau \to -\infty$, implying $C = iH/\sqrt{2k^3}$. Thereby the full solution reads

$$h = 2H \int \frac{\mathrm{d}^3\mathbf{k}}{(4\pi k)^{3/2}} \left[(i - k\tau) w_{\mathbf{k}}\, e^{-ik\tau + i\mathbf{k}\cdot\mathbf{x}} - (i + k\tau) w^\dagger_{\mathbf{k}}\, e^{ik\tau - i\mathbf{k}\cdot\mathbf{x}} \right] . \tag{3.11}$$

As a final step, we consider the equal-time correlation function. Making use of eq. (3.3), eq. (3.11) yields

$$\langle 0|\, h(\tau, \mathbf{x}_1)\, h(\tau, \mathbf{x}_2)\, |0\rangle = \int \frac{\mathrm{d}^3\mathbf{k}}{(2\pi)^3}\, e^{i\mathbf{k}\cdot(\mathbf{x}_1 - \mathbf{x}_2)}\, \frac{H^2(1 + k^2\tau^2)}{2k^3} \,. \tag{3.12}$$

The corresponding power spectrum, denoted by $\mathcal{P}_h$, is obtained by writing the integration measure as

$$\frac{\mathrm{d}^3\mathbf{k}}{(2\pi)^3} = \frac{k^3\, \mathrm{d}\ln k}{2\pi^2} \,, \tag{3.13}$$

and multiplying $k^3/(2\pi^2)$ into the integrand of eq. (3.12). This results in

$$\mathcal{P}_h = \left(\frac{H}{2\pi}\right)^2 (1 + k^2\tau^2) \overset{(3.6)}{=} \left(\frac{H}{2\pi}\right)^2 \left(1 + \frac{k^2}{a^2H^2}\right) , \tag{3.14}$$

which for $k \ll aH$ reduces to the text-book expression.

JCAP12(2022)020

3.1.2 Stochastic derivation

We proceed to repeat the computation in section 3.1.1 with another method [36], following the presentation in ref. [38]. Even if the intermediate steps look quite different, both technically and conceptually, eq. (3.14) can indeed be reproduced. As mentioned, the reason for this exercise is that it helps us to include thermal fluctuations in sections 3.2 and 3.3.

The starting point is to divide h into short-distance fluctuations ($h_<$) and a slowly varying long-distance part ($h_>$), by writing

$$h = h_> + h_< \,, \tag{3.15}$$

$$h_< \equiv \int \frac{\mathrm{d}^3\mathbf{k}}{\sqrt{(2\pi)^3}}\, W(\tau,k) \left[w_{\mathbf{k}}\, h_k(\tau)\, e^{i\mathbf{k}\cdot\mathbf{x}} + w^\dagger_{\mathbf{k}}\, h^*_k(\tau)\, e^{-i\mathbf{k}\cdot\mathbf{x}} \right] , \tag{3.16}$$

where the mode functions h_k and h^*_k are from eq. (3.10), and the window function W can be chosen as

$$W(\tau,k) \equiv \theta(k - \epsilon a H) \,. \tag{3.17}$$

The parameter ϵ drops out at the end. Inserting eq. (3.16) into eq. (3.7), we get

$$h_>'' - \frac{2}{\tau}\, h_>' - \nabla^2 h_> = \varrho_Q \,, \quad \varrho_Q \equiv -\left(\partial_\tau^2 - \frac{2}{\tau}\,\partial_\tau - \nabla^2 \right) h_< \,. \tag{3.18}$$

The subscript in ϱ_Q stands for quantum noise.

If the differential operator in ϱ_Q acts on the mode functions h_k and h^*_k in $h_<$, cf. eq. (3.16), then the result vanishes, just because this is how the mode functions have been defined. Left over are terms acting on the window function,

$$\varrho_Q(\tau,\mathbf{x}) = -\int \frac{\mathrm{d}^3\mathbf{k}}{\sqrt{(2\pi)^3}} \left[w_{\mathbf{k}}\, f_k(\tau)\, e^{i\mathbf{k}\cdot\mathbf{x}} + w^\dagger_{\mathbf{k}}\, f^*_k(\tau)\, e^{-i\mathbf{k}\cdot\mathbf{x}} \right] , \tag{3.19}$$

$$f_k(\tau) \equiv \left(W'' - \frac{2}{\tau}\, W' \right) h_k + 2 W' h_k' \,. \tag{3.20}$$

Given that W as defined by eq. (3.17) is a step function, the terms in eq. (3.20) are Dirac-δ's or their derivatives. Concretely, recalling from eq. (3.6) that $aH = -1/\tau$, we can write $W = \theta(k + \epsilon/\tau)$. A consequence from here is that $\varrho_Q(\tau_1,\mathbf{x})$ and $\varrho_Q(\tau_2,\mathbf{x})$ are commuting (i.e. classical) variables for $\tau_1 \neq \tau_2$: non-zero contributions could originate from different momenta, $k_1 \neq k_2$, but then the operators $w_{\mathbf{k}_1}$ and $w^\dagger_{\mathbf{k}_2}$ commute, cf. eq. (3.3). However, the noise represented by ϱ_Q is not obviously "white", as can be seen by determining its autocorrelator. Evaluating this in the distant-past vacuum state, we get

$$\langle 0|\, \varrho_Q(\tau_1,\mathbf{x}_1)\, \varrho_Q(\tau_2,\mathbf{x}_2)\, |0\rangle = \int \frac{\mathrm{d}^3\mathbf{k}}{(2\pi)^3}\, e^{i\mathbf{k}\cdot(\mathbf{x}_1-\mathbf{x}_2)}\, f_k(\tau_1)\, f^*_k(\tau_2) \,. \tag{3.21}$$

This is not easily simplified, given the singular nature of the structures appearing, but in practice there is no need to take further steps.

It is convenient to go to spatial momentum space,[7]

$$\langle 0|\, \varrho_Q(\tau_1,\mathbf{k})\, \varrho_Q(\tau_2,\mathbf{q})\, |0\rangle = \vec{\delta}(\mathbf{k}+\mathbf{q})\, f_k(\tau_1)\, f^*_k(\tau_2) \,. \tag{3.22}$$

[7] When we go to momentum space only in spatial directions and consider quantities which do not satisfy a classical equation of motion, the conventions are $\varrho_Q(\tau,\mathbf{k}) = \int_{\mathbf{x}} e^{-i\mathbf{k}\cdot\mathbf{x}} \varrho_Q(\tau,\mathbf{x})$ and $\varrho_Q(\tau,\mathbf{x}) = \int_{\mathbf{k}} e^{i\mathbf{k}\cdot\mathbf{x}} \varrho_Q(\tau,\mathbf{k})$, with $\int_{\mathbf{k}} \equiv \int \frac{\mathrm{d}^3\mathbf{k}}{(2\pi)^3}$. This is to be contrasted with the representation of on-shell fields, like in eq. (3.8), where a definite time dependence appears in mode functions and the momentum integration measure is different.

JCAP12(2022)020

where $\int_{\mathbf{k}} \vec{\delta}(\mathbf{k}) \equiv 1$. Equation (3.18) then becomes

$$\left(\partial_\tau^2 - \frac{2}{\tau}\,\partial_\tau + k^2 \right) h_>(\tau, \mathbf{k}) = \varrho_Q(\tau, \mathbf{k}) \,. \tag{3.23}$$

Let us solve eq. (3.23) with a retarded Green's function, denoted by $G_{\rm R}(\tau, \tau_i, k)$. It satisfies

$$\left(\partial_\tau^2 - \frac{2}{\tau}\,\partial_\tau + k^2 \right) G_{\rm R}(\tau, \tau_i, k) = \delta(\tau - \tau_i) \,, \tag{3.24}$$

with the boundary condition $G_{\rm R}(\tau, \tau_i, k) \overset{\tau<\tau_i}{\equiv} 0$. For $\tau > \tau_i$, the solution is a linear combination of the mode functions in eq. (3.10). The coefficients are obtained by integrating eq. (3.24) over the source, implying

$$\lim_{\tau \to \tau_i^+} G_{\rm R}(\tau, \tau_i, k) = 0 \,, \qquad \lim_{\tau \to \tau_i^+} \partial_\tau G_{\rm R}(\tau, \tau_i, k) = 1 \,. \tag{3.25}$$

The explicit expression reads

$$G_{\rm R}(\tau, \tau_i, k) = \frac{\theta(\tau - \tau_i)}{k^3 \tau_i^2}\, \mathrm{Im}\big[\, e^{ik(\tau - \tau_i)} (1 - ik\tau)(1 + ik\tau_i) \,\big] \,, \tag{3.26}$$

and the solution becomes

$$h_>(\tau, \mathbf{k}) = \int_{-\infty}^{\tau} \mathrm{d}\tau_i \, G_{\rm R}(\tau, \tau_i, k)\, \varrho_Q(\tau_i, \mathbf{k}) \,. \tag{3.27}$$

We now consider the equal-time correlator. In momentum space, it reads

$$\begin{aligned} \big\langle\, h_>(\tau, \mathbf{k})\, h_>(\tau, \mathbf{q}) \,\big\rangle \;&=\; \int_{-\infty}^{\tau} \mathrm{d}\tau_1 \, G_{\rm R}(\tau, \tau_1, k) \int_{-\infty}^{\tau} \mathrm{d}\tau_2 \, G_{\rm R}(\tau, \tau_2, q)\, \langle 0|\, \varrho_Q(\tau_1, \mathbf{k})\, \varrho_Q(\tau_2, \mathbf{q})\, |0\rangle \\ &\overset{(3.22)}{=} \vec{\delta}(\mathbf{k} + \mathbf{q}) \left| \int_{-\infty}^{\tau} \mathrm{d}\tau_i \, G_{\rm R}(\tau, \tau_i, k)\, f_k(\tau_i) \right|^2 . \end{aligned} \tag{3.28}$$

Inserting eq. (3.20) and carrying out a partial integration, we find

$$\begin{aligned} &\int_{-\infty}^{\tau} \mathrm{d}\tau_i \, G_{\rm R}(\tau, \tau_i, k)\, f_k(\tau_i) \\ &= \int_{-\infty}^{\tau} \mathrm{d}\tau_i \, W'(\tau_i) \left\{ -\partial_{\tau_i} G_{\rm R}(\tau, \tau_i, k) h_k(\tau_i) + G_{\rm R}(\tau, \tau_i, k) \left[h_k'(\tau_i) - \frac{2}{\tau_i}\, h_k(\tau_i) \right] \right\} . \end{aligned} \tag{3.29}$$

Making use of $aH = -1/\tau$, we can write $W'(\tau_i) = \delta(k + \frac{\epsilon}{\tau_i}) \frac{k}{\tau_i} = \delta(\tau_i - \tau_{*k})$, where τ_{*k} is the time at which the momentum mode k crosses the horizon. This then leads to

$$\int_{-\infty}^{\tau} \mathrm{d}\tau_i \, W'(\tau_i)\, \mathcal{F}(\tau_i) = \mathcal{F}(\tau_{*k}) \,. \tag{3.30}$$

It remains to insert into eqs. (3.29) and (3.30) the mode function h_k from eq. (3.10), its time derivative h_k', as well as the Green's function from eq. (3.26). There is a remarkable cancellation between many terms, so that any dependence on τ_{*k} drops out. We find

$$\int_{-\infty}^{\tau} \mathrm{d}\tau_i \, G_{\rm R}(\tau, \tau_i, k)\, f_k(\tau_i) = \frac{iH}{\sqrt{2k^3}} (1 + ik\tau) e^{-ik\tau} \overset{!}{=} h_k(\tau) \,. \tag{3.31}$$

Taking the absolute value squared, as needed in eq. (3.28), and multiplying by $k^3/(2\pi^2)$, like between eqs. (3.13) and (3.14), the power spectrum in eq. (3.14) is recovered.

JCAP12(2022)020

3.1.3 Including helicity

The helicity components of tensor perturbations of the metric, or gravitational waves, satisfy the same equation in de Sitter spacetime as the scalar fluctuations considered in sections 3.1.1 and 3.1.2. Thus, once we fix normalization, via a comparison with eq. (3.1), and take care of the sum over helicities or polarizations, the results can be extracted from above. We denote tensor perturbations of the metric by $\delta g^{\mathrm{t}i}{}_j \equiv h^{\mathrm{t}}_{ij}$, with the convention that spatial indices are raised and lowered like in flat spacetime, i.e. $T_{ij} \equiv T^{ij} \equiv T^i{}_j$.

In a local Minkowskian frame, the energy associated with tensor perturbations reads

$$\left[\, E_{\scriptscriptstyle \mathrm{GW}} \,\right]_{\scriptscriptstyle M} = \frac{1}{32\pi G} \int \mathrm{d}^3\mathbf{y}\, (\dot{h}^{\mathrm{t}}_{ij})^2 \,. \tag{3.32}$$

If we express a wave as a linear combination of forward and backward propagating modes, and integrate over a time larger than the oscillation period, so that fast oscillations $e^{\pm 2ipt}$ average out, then eq. (3.32) can be substituted through

$$\left\langle\, E_{\scriptscriptstyle \mathrm{GW}} \,\right\rangle_{\scriptscriptstyle M} = \frac{1}{32\pi G} \int \mathrm{d}^3\mathbf{y}\, \frac{1}{2} \left[\, (\dot{h}^{\mathrm{t}}_{ij})^2 + (\nabla h^{\mathrm{t}}_{ij})^2 \,\right] . \tag{3.33}$$

Comparing with eq. (3.1), canonically normalized tensor modes, denoted in the following by $\hat{h}^{\mathrm{t}}_{ij}$, are obtained as $\hat{h}^{\mathrm{t}}_{ij} \equiv h^{\mathrm{t}}_{ij}/\sqrt{32\pi G}$.

There are two propagating helicity states in the tensor channel. Denoting the normalized and complete set of polarization tensors by ϵ^{λ}_{ij}, we may write in momentum space

$$\hat{h}^{\mathrm{t}}_{ij} = \sum_{\lambda} \epsilon^{\lambda}_{ij}\, \hat{h}^{\lambda} \,, \quad \sum_{i,j} \epsilon^{\lambda}_{ij}\, \epsilon^{\lambda' *}_{ij} = \delta^{\lambda\lambda'} \,. \tag{3.34}$$

For the same momentum, each state obeys the same equation and carries the same energy density. Therefore the power spectrum $\mathcal{P}_{\mathrm{T}}$, associated with $\sum_\lambda h^\lambda$, becomes

$$\mathcal{P}_{\mathrm{T}}(k) = \underbrace{32\pi G}_{h^2/\hat{h}^2} \times \underbrace{2}_{\sum_\lambda} \times \underbrace{\left(\frac{H}{2\pi}\right)^2 \left(1 + \frac{k^2}{a^2H^2}\right)}_{(3.14)} = \frac{16}{\pi}\left(\frac{H}{m_{\mathrm{pl}}}\right)^2 \left(1 + \frac{k^2}{a^2H^2}\right) . \tag{3.35}$$

As for the practical use of eq. (3.35), we recall that during inflation, H is approximately constant whereas a grows rapidly (k is constant by definition). Conventionally, $\mathcal{P}_{\mathrm{T}}(k)$ is evaluated at horizon crossing, with $k = aH$. Taken literally, the second term in eq. (3.35) would then represent a 100% correction, but this is an illusion, as a short moment later it would be minuscule, whereas the first term would remain intact. Therefore, we can adopt the standard convention $k = aH$ for horizon crossing, with the implicit understanding that the second term in eq. (3.35) needs to be omitted, recovering the standard literature result.

3.2 Thermal fluctuations

Apart from vacuum fluctuations, tensor modes can also be produced by thermal ones, via the Einstein equation

$$(\,\partial_\tau^2 + 2\mathcal{H}\,\partial_\tau - \nabla^2\,) h^{\mathrm{t}}_{ij} = 16\pi G a^2\, T^{\mathrm{t}}_{ij} \,, \tag{3.36}$$

where T^{t}_{ij} is the tensor part of a matter energy-momentum tensor. Even if the average value of T^{t}_{ij} vanishes, non-zero values are produced by fluctuations. At large wavelengths (small momenta), the latter are known as hydrodynamic fluctuations. Though this is in principle

JCAP12(2022)020

a text-book topic, the treatment of hydrodynamic fluctuations often does not belong to our standard tool kit. It turns out that for the tensor modes, the story is simpler than for scalar and vector modes, and we recall here the basic ingredients.

In the hydrodynamic domain, the energy-momentum tensor is expressed in terms of a gradient expansion operating on macroscopic variables, namely the local temperature, T, and the local fluid velocity, v_i. The zeroth order contains no gradients, and is known as ideal hydrodynamics, with the dependence on T parametrized through a local energy density and pressure (e and p, respectively). At first order in gradients, the dependence on T is parametrized by two new quantities, the shear and bulk viscosities (η and ζ, respectively). Crucially, at the same order, hydrodynamic fluctuations need to be included [39]. The underlying reason is the fluctuation-dissipation theorem: viscosities are dissipative coefficients, which transfer energy from fluid motion to thermal noise. This must be compensated for by fluctuations, returning energy from thermal noise to the fluid degrees of freedom.

Concretely, at first order in gradients, the energy-momentum tensor can be expressed as

$$T^{\mu\nu}_{\rm hydro} = \bar{T}^{\mu\nu}_{\rm hydro} + \delta T^{\mu\nu}_{\rm hydro} + S^{\mu\nu} + \mathcal{O}(\delta^2) \,. \tag{3.37}$$

Here $\bar{T}^{\mu\nu}_{\rm hydro}$ contains the average values of the hydrodynamic variables ($T \equiv \bar{T}, \bar{v}_i \equiv 0$), $\delta T^{\mu\nu}_{\rm hydro}$ their expansions to first order ($\delta T, v_i \equiv \delta v_i$), and $S^{\mu\nu}$ the fluctuations. At first order, recalling our convention that spatial indices are raised and lowered with δ^{ij} and δ_{ij}, the fluctuation autocorrelator has the form [39, 40]

$$\langle\, S^{ij}(\mathcal{X})\, S^{mn}(\mathcal{Y})\,\rangle = 2T\left[\eta\,(\delta_{im}\delta_{jn}+\delta_{in}\delta_{jm}) + \left(\zeta - \frac{2\eta}{3}\right)\delta_{ij}\delta_{mn}\right]\frac{\delta(\mathcal{X}-\mathcal{Y})}{\sqrt{-\det g_{\mu\nu}}} \,. \tag{3.38}$$

Only the spatial part displays non-vanishing correlators at this order.

Now, when we consider the production of tensor perturbations, we go to momentum space in the spatial directions, and sum over the graviton polarization states. With the notation from eq. (3.34), the latter produces

$$\sum_\lambda \epsilon^\lambda_{ij}\,\epsilon^{\lambda *}_{mn} = \mathbb{L}_{ij;mn} \,, \tag{3.39}$$

$$\mathbb{L}_{ij;mn} \equiv \frac{\mathbb{P}^{\rm T}_{im}\mathbb{P}^{\rm T}_{jn} + \mathbb{P}^{\rm T}_{in}\mathbb{P}^{\rm T}_{jm} - \mathbb{P}^{\rm T}_{ij}\mathbb{P}^{\rm T}_{mn}}{2} \,, \quad \mathbb{P}^{\rm T}_{ij} \equiv \left(\delta_{ij} - \frac{k_i k_j}{k^2}\right) . \tag{3.40}$$

The 2-point function of tensor fluctuations of the energy-momentum tensor thus contains

$$\begin{aligned}
&\mathbb{L}_{ij;mn}\Big\langle\, T^{ij}_{\rm hydro}(\tau_1,\mathbf{k}) T^{mn}_{\rm hydro}(\tau_2,\mathbf{q})\,\Big\rangle \\
&= \mathbb{L}_{ij;mn}\Big\langle\, [\delta T^{ij}_{\rm hydro} + S^{ij}](\tau_1,\mathbf{k})\,[\delta T^{mn}_{\rm hydro} + S^{mn}](\tau_2,\mathbf{q})\,\Big\rangle \\
&= \mathbb{L}_{ij;mn}\Big\langle\, S^{ij}(\tau_1,\mathbf{k})\, S^{mn}(\tau_2,\mathbf{q})\,\Big\rangle \\
&= \frac{8T\eta\,\delta(\mathbf{k}+\mathbf{q})\,\delta(\tau_1-\tau_2)}{a^4} \,.
\end{aligned} \tag{3.41}$$

In the penultimate step we made use of the fact that $\delta T^{ij}_{\rm hydro}$ has no projection onto tensor modes, so that the correlator arises directly from the fluctuations. Let us remark that the projection could be carried out without a helicity sum as well, yielding then $8T\eta \to 4T\eta\,\delta^{\lambda\lambda'}$.

JCAP12(2022)020

In order to make use of eq. (3.41), we need to know the value of the shear viscosity. In a system with a thermalized inflaton coupled to a heat bath through a damping coefficient Υ, the value of the shear viscosity emanating from Υ can be obtained from eq. (3.19) of ref. [22], by converting the imaginary part of the retarded correlator to a statistical (time-symmetric) correlator and taking the IR limit,

$$T\eta \supset T\eta_\chi \equiv \lim_{\omega,k\to 0} \frac{T\,\mathrm{Im}\,G^{\mathrm{R}}_{xy;xy}(\omega,k)}{\omega} = \int_{\mathbf{p}} \frac{p_x^2 p_y^2\, n_{\mathrm{B}}(\epsilon_p)[1+n_{\mathrm{B}}(\epsilon_p)]}{\Upsilon\,\epsilon_p^2}\,, \quad \epsilon_p^2 \equiv p^2+m^2\,. \tag{3.42}$$

This shows how a weak coupling leads to a large shear viscosity, a phenomenon that we can physically associate with a long mean free path. However, the shear viscosity gets contributions also from reactions not involving the inflaton; in a pure gauge plasma, it reads [41]

$$T\eta \supset T\eta_{\mathrm{gauge}} \overset{\substack{N_{\mathrm{c}}=3\\ N_{\mathrm{f}}=0}}{\simeq} \frac{27.126\,T^4}{g^4\ln\!\left(\frac{2.765\,T}{m_{\mathrm{D}}}\right)}\,, \quad m_{\mathrm{D}}^2 = \frac{g^2T^2}{3}\,. \tag{3.43}$$

For $T \gg m$, eq. (3.42) dominates, as $\Upsilon \ll \epsilon_p$ can be very small compared with T; for $T \ll m$, eq. (3.43) turns into the leading contribution, given that eq. (3.42) is suppressed by $e^{-m/T}$.

3.3 Combining vacuum and thermal fluctuations

In the warm inflation literature, it is often stated that there are no thermal corrections to tensor perturbations, unless gravitons get thermalized, which is unlikely (see below). That said, thermal corrections were addressed in ref. [42], and argued to be possibly important; at the same time, the vacuum part was omitted from the formalism, even if at the end the thermal contribution was compared with it. The approach below largely agrees with that of ref. [42], but incorporates the vacuum part all along and does not assume de Sitter spacetime.

Let us first briefly contrast with scalar perturbations. These are damped by the coefficient Υ appearing in eq. (3.42), and excited by thermal noise [31]. In principle, tensor perturbations also experience damping, with an associated coefficient Υ^{t}. However, for physical momenta $k/a \lesssim \alpha^2 T$, Υ^{t} is proportional to the shear viscosity η, divided by m_{pl}^2, and in total of order $\Upsilon^{\mathrm{t}} \sim T^3/(\alpha^2 m_{\mathrm{pl}}^2)$ [43]. This is normally smaller than the Hubble rate, $\Upsilon^{\mathrm{t}} \ll H \sim T^2/m_{\mathrm{pl}}$. Therefore gravitons are not damped or thermalized: Υ^t can be omitted, and we associate no Bose distribution to gravitons.

Going to momentum space, multiplying eq. (3.36) with the polarization vector ϵ_{ij}^λ, and summing over the spatial indices, we find

$$(\,\partial_\tau^2 + 2\mathcal{H}\,\partial_\tau + k^2\,)h^\lambda(\tau,\mathbf{k}) = 16\pi G a^2 \sum_{i,j} \epsilon_{ij}^\lambda T_{ij}^{\mathrm{t}}(\tau,\mathbf{k}) \equiv \varrho_T^\lambda(\tau,\mathbf{k})\,. \tag{3.44}$$

Dividing h^λ into short-distance fluctuations and a slowly varying part, like in eq. (3.15), the evolution equation for the latter can then be expressed as

$$(\,\partial_\tau^2 + 2\mathcal{H}\,\partial_\tau + k^2\,)h_>^\lambda(\tau,\mathbf{k}) = (\,\varrho_Q^\lambda + \varrho_T^\lambda\,)(\tau,\mathbf{k})\,. \tag{3.45}$$

Recalling the connection of h^λ to canonically normalized fields, like below eq. (3.33), the autocorrelator of the vacuum fluctuations in eq. (3.22) takes the form

$$\langle\, \varrho_Q^\lambda(\tau_1,\mathbf{k})\,\varrho_Q^{\lambda'}(\tau_2,\mathbf{q})\,\rangle = \delta(\mathbf{k}+\mathbf{q})\,\delta^{\lambda\lambda'} f_k(\tau_1)\,f_k^*(\tau_2)\,32\pi G\,. \tag{3.46}$$

JCAP12(2022)020

For the thermal noise autocorrelator, the definition in eq. (3.44) together with the hydrodynamic noise in eq. (3.41) imply that

$$\langle\, \varrho_T^{\lambda}(\tau_1, \mathbf{k})\, \varrho_T^{\lambda'}(\tau_2, \mathbf{q})\,\rangle = \delta(\mathbf{k}+\mathbf{q})\, \delta^{\lambda\lambda'}\, \delta(\tau_1 - \tau_2)\, 4T(\tau_1)\, \eta(\tau_1)\, (16\pi G)^2\,. \tag{3.47}$$

The mixed noise correlator vanishes, since the impact of gravitational waves on the thermal plasma, or vice versa, is suppressed by higher powers of G.

Solving eq. (3.45) with Green's functions, cf. eq. (3.26), and recalling that there are two polarization states, the power spectrum at a time τ_e finally becomes

$$\mathcal{P}_{\mathrm{T}}(k) = \frac{64\pi G\, k^3}{2\pi^2} \left\{ \left| \int_{-\infty}^{\tau_e} \mathrm{d}\tau_i\, G_{\mathrm{R}}(\tau_e, \tau_i, k)\, f_k(\tau_i) \right|^2 + 32\pi G \int_{-\infty}^{\tau_e} \mathrm{d}\tau_i\, G_{\mathrm{R}}^2(\tau_e, \tau_i, k)\, T(\tau_i)\, \eta(\tau_i) \right\}. \tag{3.48}$$

Here we have introduced the notation τ_e for some arbitrarily chosen moment shortly after inflation, such that $k/(a_e H_e) \ll 1$ for the momenta that affect phenomenological predictions today (cf. section 3.4). In the slow-roll regime the first part of eq. (3.48) can be simplified, cf. eq. (3.31), but the second part not, because T and η can be complicated functions of time, and because their dominant contribution can originate at a late time when de Sitter is no longer a good approximation.

We note from eq. (3.48) that the thermal contribution to the tensor power spectrum is suppressed by $1/m_{\mathrm{pl}}^2$ compared with the vacuum contribution. However, while the vacuum contribution is localized in time, originating when the modes cross the horizon, this is not necessarily the case for the thermal contribution, which can continue for a while, thereby compensating for the apparent suppression.

3.4 From primordial spectrum to the current gravitational energy density

The current-day observable corresponding to $\mathcal{P}_{\mathrm{T}}$ is the power spectrum of the fractional energy density carried by gravitational waves, denoted by Ω_{GW} and defined in eq. (3.52). We recall here how the transfer function from $\mathcal{P}_{\mathrm{T}}$ to Ω_{GW} can be obtained, following the presentation in refs. [44, 45] (early work can be found in ref. [46]).

The starting point is the energy in eq. (3.32), averaged like in eq. (3.33). We simultaneously take a vacuum and thermal average, like in eqs. (3.46) and (3.47). Furthermore we make use of translational invariance, dividing by volume and thereby defining the energy density. Going over to conformal time, the energy density today ($\tau \to \tau_0$, $a \to a_0$) reads

$$e_{\mathrm{GW}}(\tau_0) = \frac{1}{32\pi G a_0^2} \sum_{i,j} \langle\, h_{ij}^{\mathrm{t}\,\prime}(\tau_0, \mathbf{y})\, h_{ij}^{\mathrm{t}\,\prime}(\tau_0, \mathbf{y})\,\rangle\,, \tag{3.49}$$

where the left-hand side does not depend on $\mathbf{y}$ because of translational invariance. The energy density in eq. (3.49) can be compared with the total energy density today (cf. eq. (2.3)),

$$e_{\mathrm{crit}} \equiv e_r(\tau_0) = \frac{3H_0^2}{8\pi G}\,, \tag{3.50}$$

where the current Hubble rate is conventially expressed as $H_0 = 100\, h$ km s^{-1} Mpc^{-1}.

We now adopt co-moving Fourier space in spatial directions, and represent the tensor structure in the helicity basis, like in eq. (3.34). The tensor perturbation is written as a

JCAP12(2022)020

functional[8] of its initial value at the end of inflation,

$$h^{\lambda}(\tau_0,k) \equiv X(\tau_0,\tau_e,k)\, h^{\lambda}(\tau_e,k)\;, \quad X(\tau_e,\tau_e,k) \equiv 1\;, \quad \partial_{\tau_0} X(\tau_0,\tau_e,k) \overset{\tau_0=\tau_e}{=} 0\;. \tag{3.51}$$

This leads to

$$\Omega_{\scriptscriptstyle\rm GW}(k) \equiv \frac{1}{e_{\rm crit}} \frac{\mathrm{d}e_{\scriptscriptstyle\rm GW}(\tau_0)}{\mathrm{d}\ln k} = \frac{[\partial_{\tau_0} X(\tau_0,\tau_e,k)]^2 \mathcal{P}_{\scriptscriptstyle\rm T}(k)}{32\pi G a_0^2\, e_{\rm crit}} = \underbrace{\frac{[\partial_{\tau_0} X(\tau_0,\tau_e,k)]^2}{12 a_0^2 H_0^2}}_{\equiv \mathcal{T}_{\scriptscriptstyle\rm T}(k)} \mathcal{P}_{\scriptscriptstyle\rm T}(k)\;, \tag{3.52}$$

where $\mathcal{T}_{\scriptscriptstyle\rm T}(k)$ is called the transfer function in the tensor channel. Normally, $\Omega_{\scriptscriptstyle\rm GW}$ is expressed in terms of the current-day frequency, f_0, as $\Omega_{\scriptscriptstyle\rm GW}(f_0)$.

Given that $\mathcal{T}_{\scriptscriptstyle\rm T}$ accounts for physics after the reheating period, thermodynamic functions are dominated by their radiation parts. The average energy density, pressure, entropy density, and heat capacity satisfy standard relations, $s_r = \partial_T p_r$, $e_r = T s_r - p_r$, $c_r \equiv \partial_T e_r = T \partial_T s_r$. We also make use of the speed of sound squared, $c_s^2 \equiv \partial_T p_r / \partial_T e_r = s_r / c_r$. Unlike for inflation, where an SU($N_{\rm c}$) gauge plasma was assumed to constitute the heat bath, we include the full Standard Model in these post-inflationary thermodynamic functions.

For tracking the evolution of the temperature, it is helpful to employ the variable

$$z \equiv \ln\!\left(\frac{T_e}{T}\right)\;, \tag{3.53}$$

where T_e denotes the temperature at the end of inflation. In practice we have chosen $T_e \equiv 10^{-9} m_{\rm pl} = 1.22091 \times 10^{10}\,\mathrm{GeV}$, but this is just a convention and has no physical effect.

Now, the scale factor, a, can be expressed in terms of z. In the absence of $\bar{\varphi}$, the background equation, eq. (2.2), can be written as $e_r' = -3\mathcal{H}(e_r + p_r)$, which after the insertion of the thermodynamic identities turns into

$$\left(\, s_r a^3 \,\right)' = 0\;. \tag{3.54}$$

From here we get

$$a = a_e \left(\frac{s_e}{s_r}\right)^{1/3}\;, \quad \mathcal{H} = \sqrt{\frac{8\pi e_r}{3}}\, \frac{a_e}{m_{\rm pl}} \left(\frac{s_e}{s_r}\right)^{1/3}\;. \tag{3.55}$$

In addition eq. (3.54) gives an evolution equation for z itself,

$$\partial_u z = \frac{3 c_s^2\, \mathcal{H}}{k}\;, \quad u \equiv k\tau\;, \tag{3.56}$$

where we made use of thermodynamic identities and introduced the helpful variable u [47]. Using eq. (3.51) in eq. (3.45) and neglecting the right-hand side,[9] X in turn satisfies

$$\partial_u^2 X + \frac{2\mathcal{H}\partial_u X}{k} + X = 0\;, \quad u > u_e\;. \tag{3.57}$$

[8] Given that h^{λ} obeys a second order differential equation, both its initial value and time derivative are needed for specifying the solution. The notation assumes that τ_e is chosen at a moment where the conformal time derivative vanishes, because the modes are well outside the horizon. For simplicity we also envision that the system has reheated by this time, i.e. that the energy density is dominated by radiation.

[9] The physics of "neutrino free streaming" in a gravitational wave background after their decoupling (cf. ref. [47] and references therein) induces an additional term in the equation, but it only affects frequencies $f_0 \lesssim 10^{-9}$ Hz [44]. These are far below the LISA window and thus not relevant for us here.

JCAP12(2022)020

In order to solve eqs. (3.56) and (3.57), we need to know the evolution of the ratio $k/\mathcal{H}$. Co-moving momenta are conveniently parametrized by the current frequency, f_0/Hz. Let us express k in terms of the physical momentum evaluated at present time, p_0, as $k = a_0\, p_0$. In natural units ($\hbar = c = k_{\mathrm{B}} = 1$), $p_0 = \omega_0 = 2\pi f_0$. Making use of eq. (3.54), we may then write

$$\frac{k}{\mathcal{H}} = \frac{k}{aH} = \frac{a_0 p_0}{aH} = \frac{p_0}{T_0}\left(\frac{a_0^3 T_0^3}{a^3 T^3}\right)^{\frac{1}{3}} \frac{T}{H} = \underbrace{\frac{2\pi}{\mathrm{s}\, T_0}\sqrt{\frac{3}{8\pi}}}_{\approx\, 6.0837\times 10^{-12}} \left(\frac{s_r/T^3}{s_0/T_0^3}\right)^{\frac{1}{3}} \frac{m_{\mathrm{pl}}/T}{\sqrt{e_r/T^4}}\, \frac{f_0}{\mathrm{Hz}}\,. \tag{3.58}$$

Tabulated results for c_s^2 (for eq. (3.56)) as well as s_r/T^3 and e_r/T^4 (for eq. (3.58)) can be found in ref. [48].[10]

We recall in passing that the number of e-folds in the postinflationary epoch reads

$$\ln\!\left(\frac{a_0}{a_e}\right) = \ln\!\left(\frac{T_e}{\mathrm{GeV}}\,\frac{10^9}{(T_0/\mathrm{K})(k_{\mathrm{B}}\mathrm{K}/\mathrm{eV})}\right) + \frac{1}{3}\ln\!\left(\frac{s_e/T_e^3}{s_0/T_0^3}\right) \;\approx\; 53.4\,. \tag{3.60}$$

The end of inflation, T_e, is chosen at a later moment than when the maximal temperature, T_{max}, had been reached. For a physical result, we should add the e-folds between T_e and T_{max}, which for the benchmark shown in figure 3 gives $\Delta N \simeq 4$. In total the thermal epoch therefore amounts to $N_{\mathrm{thermal}} \simeq 57$ e-folds. To compensate for this, i.e. to guarantee that the modes which have re-entered the horizon just recently, were causally connected before inflation, it is customary to require that the inflationary period extended for at least ~ 60 e-folds before reaching T_{max}, and we adopt this convention in the following.[11]

Returning to eq. (3.57), the last term plays little role when $k/\mathcal{H} \ll 1$, and the solution stays close to the initial value $\partial_u X = 0$. Once a mode re-enters the horizon, so that $k/\mathcal{H} \gg 1$, the last term dominates, and rapid oscillations set in. Their precise treatment requires care. For a fixed f_0/Hz, we first follow eq. (3.58) from low temperatures up to T_e, to see if the mode was outside the horizon in the first place. If yes, we integrate from $u = u_e$ up to a point where $k/\mathcal{H} = 30$, resulting in $30/(2\pi) \sim 5$ oscillations.[12] At this point, following ref. [45], we match onto the asymptotic $u \gg 1$ solution, used for extrapolating to the present time.

Let us express the asymptotic solution, valid for $k^2 \gg a''/a$, as

$$X \approx \alpha\, \frac{a_m}{a}\sin(u - u_m + \beta)\,, \tag{3.61}$$

where $u_m > u_e$ denotes the matching point, a_m the scale factor at that point, and α and β are integration constants. The latter can be matched onto X and $\partial_u X$ at u_m,

$$\beta = \arctan\!\left\{\left(\frac{\mathcal{H}}{k} + \frac{\partial_u X}{X}\right)^{-1}\right\}_{u=u_m}\,, \quad \alpha = \frac{X(u_m)}{\sin\beta}\,. \tag{3.62}$$

[10] The dimensionless prefactor in eq. (3.58) can be written as

$$\frac{2\pi}{\mathrm{s}\, T_0}\sqrt{\frac{3}{8\pi}} = \sqrt{\frac{3\pi}{2}}\,\frac{\hbar/(\mathrm{eVs})}{(T_0/\mathrm{K})(k_{\mathrm{B}}\mathrm{K}/\mathrm{eV})}\,, \tag{3.59}$$

where $\hbar = 6.582119569\times 10^{-16}\,\mathrm{eVs}$, $T_0 \approx 2.7255\,\mathrm{K}$, and $k_{\mathrm{B}}K = 8.617333262\times 10^{-5}\,\mathrm{eV}$.

[11] In our benchmark, the CMB frequencies $f_0 = (10^{-19}\text{–}10^{-16})\,\mathrm{Hz}$, corresponding to the wave numbers in footnote 1, crossed the horizon $\Delta N = 59 - 52$ e-folds before the solution reached T_{max}, respectively.

[12] As long as the matching point satisfies $k/\mathcal{H} \geq 20$, the results are independent of the choice.

JCAP12(2022)020

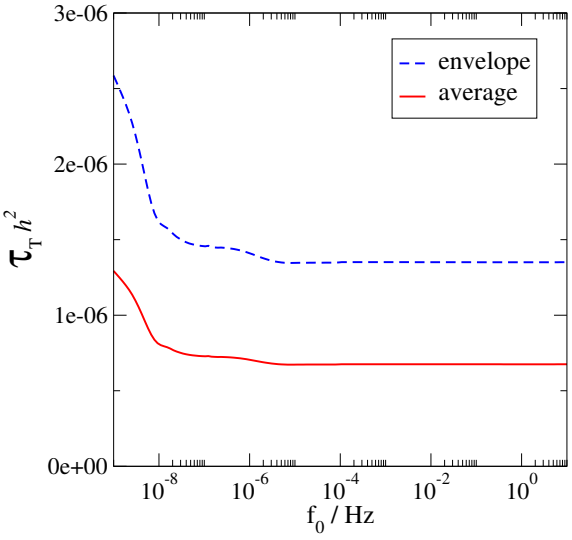

Figure 1. The transfer function from eq. (3.64). The dashed line shows the envelope ($\cos^2 \to 1$) and the solid line the average ($\cos^2 \to \frac{1}{2}$) of rapid oscillations. The feature at $f_0 \sim 10^{-8}\,\mathrm{Hz}$ originates from the QCD crossover, treated according to ref. [49]; the smooth features at $f_0 \sim 10^{-6}\,\mathrm{Hz}$ are related to the crossing of mass thresholds [49]; whereas the electroweak crossover, treated according to ref. [50], leaves behind an almost invisible shape at $f_0 \sim (3-4)\times 10^{-4}\,\mathrm{Hz}$.

Inserting eq. (3.61) and keeping only the dominant term at $k \gg \mathcal{H}$, the transfer function from eq. (3.52) becomes

$$\mathcal{T}_{\mathrm{T}} \;\approx\; \frac{\alpha^2}{12}\left(\frac{k}{a_0 H_0}\right)^2 \left(\frac{s_0}{s_m}\right)^{2/3} \cos^2(u_0 - u_m + \beta)\;. \tag{3.63}$$

Like in eq. (3.58), we write $k = 2\pi a_0 f_0$, and insert then coefficients like in eq. (3.59),[13]

$$\mathcal{T}_{\mathrm{T}}\, h^2 \;\approx\; \frac{\alpha^2}{12}\left(\frac{f_0}{\mathrm{Hz}}\right)^2 \Bigg(\underbrace{\frac{2\pi[hc/(\mathrm{m}H_0)](T_0/\mathrm{K})(k_{\mathrm{B}}\mathrm{K}/\mathrm{eV})}{10^9(cs/\mathrm{m})}}_{\approx 4.5535\times 10^5}\Bigg)^2 \left(\frac{\mathrm{GeV}}{T_m}\right)^2 \left(\frac{s_0/T_0^3}{s_m/T_m^3}\right)^{2/3} \cos^2(\ldots)\;. \tag{3.64}$$

Even if α, T_m and s_m depend on the matching point, the final result is independent of it.

Rather than showing the rapid oscillations from eq. (3.64), we plot their envelope ($\cos^2 \to 1$) and average ($\cos^2 \to \frac{1}{2}$), with a result that can be found in figure 1. According to eq. (3.52), this determines the relation between $\mathcal{P}_{\mathrm{T}}$ at $T = T_e$, and Ω_{GW} at the present time.

4 Analytical and numerical results

The purpose of this section is to illustrate the theoretical results of section 3 with semi-realistic parameter values. We first carry out a parameter scan of CMB constraints for the potential of eq. (1.2) (cf. section 4.1); analyse the corresponding gravitational wave predictions in the LISA frequency window (cf. section 4.2); and turn then to other potentials (cf. section 4.3).

[13] Here the further values $hc/(\mathrm{m}H_0) \approx 0.9250629 \times 10^{26}$ and $cs/\mathrm{m} = 2.99792458 \times 10^8$ were needed.

JCAP12(2022)020

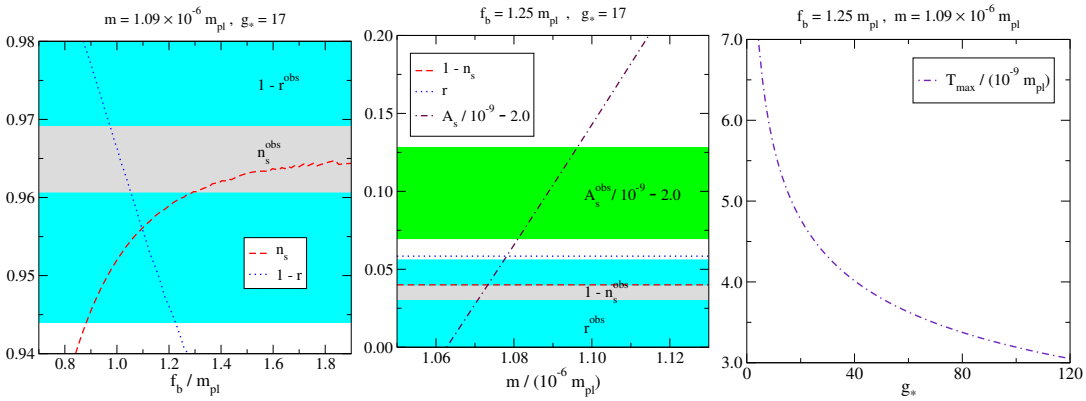

Figure 2. The observables A_s, n_s and r (cf. eqs. (4.1)–(4.3)) as a function of $f_b/m_{\rm pl}$ (left) and $m/(10^{-6}\,m_{\rm pl})$ (middle) for the potential in eq. (1.2). The parameters not varied have been set to the benchmark values $f_b = 1.25\,m_{\rm pl}$, $m = 1.09\times10^{-6}\,m_{\rm pl}$ and $g_* = 17$. The bands show the 1σ (68% CL) contours [2]. The right panel illustrates the maximal temperature, as a function of g_*.

4.1 Scan of parameter space

As the background solution (cf. section 2) turns out to be in a weak regime of warm inflation (i.e. with $\Upsilon \ll H$) at the time when CMB perturbations are generated, we adopt vacuum predictions for scalar perturbations. This also concerns tensor perturbations in the frequency domain relevant for CMB predictions, i.e. $f_0 \ll 10^{-15}\,$Hz. The standard expressions read

$$A_s \equiv \mathcal{P}_{\mathcal{R}}(k)\big|_{H_*} \approx \left(\frac{H_*^2}{2\pi\dot\varphi}\right)^2 , \tag{4.1}$$

$$n_s \equiv 1 + \frac{\mathrm{d}\ln\mathcal{P}_{\mathcal{R}}(k)}{\mathrm{d}\ln k}\bigg|_{H_*} \approx 1 + \frac{2H_*}{H_*^2+\dot H_*}\left(\frac{2\dot H_*}{H_*} - \frac{\ddot\varphi}{\dot\varphi}\right) , \tag{4.2}$$

$$r \equiv \frac{\mathcal{P}_{\rm T}(k)}{\mathcal{P}_{\mathcal{R}}(k)}\bigg|_{H_*} \approx 4\pi G\left(\frac{4\dot\varphi}{H_*}\right)^2 , \tag{4.3}$$

where $\mathcal{R}$ denotes a curvature perturbation, k is chosen as a typical CMB co-moving momentum, and H_* is the Hubble rate at the time when this mode first exits the horizon ($k = a_*H_*$). In terms of slow-roll parameters, *viz.*

$$\epsilon_V \equiv \frac{1}{16\pi G}\left(\frac{V_\varphi}{V}\right)^2 , \quad \eta_V \equiv \frac{1}{8\pi G}\frac{V_{\varphi\varphi}}{V} , \tag{4.4}$$

eqs. (4.1)–(4.3) can be approximated as

$$A_s \approx \frac{128\pi G^3}{3}\frac{V^3}{V_\varphi^2} = \frac{8G^2V}{3\epsilon_V} , \tag{4.5}$$

$$n_s \approx 1 + \frac{\dot\varphi}{H_*}\frac{\epsilon_V}{V}\,\partial_\varphi\left(\frac{V}{\epsilon_V}\right) \approx 1 - 6\epsilon_V + 2\eta_V , \tag{4.6}$$

$$r \approx 64\pi G\left(\frac{V_\varphi}{8\pi G V}\right)^2 = 16\epsilon_V . \tag{4.7}$$

By convention we evaluate these $N = 60$ e-folds before the solution reaches the maximal temperature (cf. footnote 11), whose value is plotted in figure 2 (right).

JCAP12(2022)020

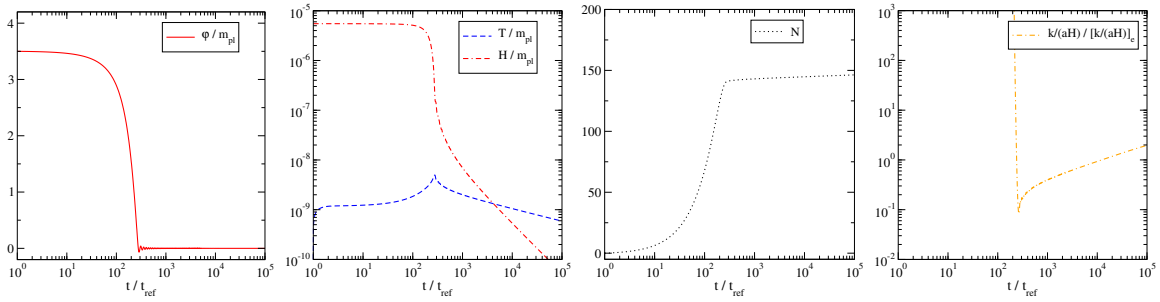

Figure 3. A benchmark solution extracted from the scans of figure 2, for $f_b = 1.25\, m_{\rm pl}$, $m = 1.09 \times 10^{-6}\, m_{\rm pl}$ and $g_* = 17$, which lies within 2σ of the observational constraints [2]. The initial values have been set to $\varphi(t_{\rm ref}) = 3.5\, m_{\rm pl}$ and $T(t_{\rm ref}) = 10^{-10}\, m_{\rm pl}$, where $t_{\rm ref}^{-1} \equiv \sqrt{\frac{4\pi}{3}} \frac{m\varphi(t_{\rm ref})}{m_{\rm pl}}$. In the last panel, $k/(aH)$ from eq. (2.5) has been normalized to an "endpoint of inflation", $t_e \approx 1.2 \times 10^4 t_{\rm ref}$ (cf. eq. (3.53)); for $t > t_e$ we use the Standard Model radiation solution for $k/(aH)$, given in eq. (3.58). We remark that $T(t_{\rm ref})$ is quite large, chosen in order not to miss a possible strong regime of warm inflation, however the solution is an attractor, so that the initial value does not affect the later behaviour.

We note that if we employ a potential with the shape of eq. (1.2), then the mass squared drops out in the slow-roll parameters ϵ_V and η_V from eq. (4.4). Once we fix the initial field value, $\bar{\varphi}(t_{\rm ref})$, close enough to the maximum of the potential, so that sufficiently many e-folds take place before reheating, then n_s and r depend only on f_b. This dependence is shown in figure 2 (left), and permits for us to fix $f_b/m_{\rm pl}$.[14] Subsequently, $m/m_{\rm pl}$ can be fixed by considering A_s, as can be seen from figure 2 (middle). Two issues should be kept in mind, however: A_s depends strongly on the number of e-folds considered; and radiative corrections to the scalar mass, proportional to couplings of the scalar and to powers of H^2, could be substantial in de Sitter spacetime (cf. the discussion in the second paragraph of section 2). Therefore the value of $m/m_{\rm pl}$ is to be considered as a qualitative indication only.

A benchmark solution for parameters extracted from the scans is illustrated in figure 3.

4.2 Shape of the gravitational wave background

The purpose of this section, which is the key part of our study, is to determine the gravitational wave background that originates from a solution like in figure 3. Instead of the very small frequencies $f_0 \ll 10^{-15}\,$Hz that affect the parameter r, we now move to larger frequencies, in and around the LISA window $f_0 \sim (10^{-4}\text{–}10^{-1})\,$Hz. To set this exercise in context, we note that a similar study for another model can be found in ref. [51] (an UV contribution viable to very large frequencies, $f_0 \gg 10^6\,$Hz, was added in ref. [52]).

For a general overview, let us recall that different contributions to $\Omega_{\rm GW}(f_0)$ lead to qualitatively different f_0-shapes:

(i) The contribution from vacuum fluctuations during inflation leads to a flat spectrum at small frequencies, eq. (3.35). The flat spectrum is slightly modified by the decreasing Hubble rate (this is illustrated in figure 4) as well as the post-inflationary transfer function (cf. figure 1). Altogether these effects lead to a spectral tilt $n_{\rm T}$, one of the parameters that can conceivably be constrained with LISA [7]. Unfortunately, the overall amplitude is below the LISA observation threshold (cf. the caption of figure 4).

[14] In contrast to ref. [27], we always set $f_a = f_b$, whereby thermal effects are quite different.

JCAP12(2022)020

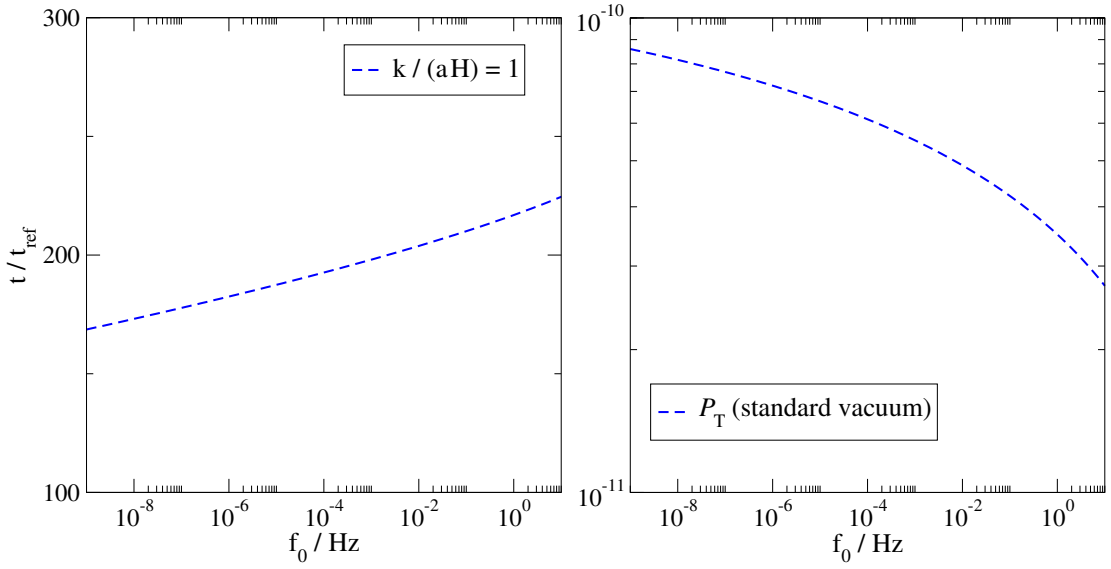

Figure 4. Left: for the solution shown in figure 3, the time at which a given momentum mode crosses the horizon for the first time, i.e. $k = aH$. Right: the vacuum contribution to the primordial tensor spectrum from eq. (3.35), originating at this moment. The non-trivial shape stems from the fact that large frequencies cross the horizon at a time when the Hubble rate is already decreasing (cf. the second panel in figure 3). For physical predictions, $\mathcal{P}_{\mathrm{T}}$ needs to be multiplied with the transfer function from figure 1, cf. eq. (3.52), yielding a value $\Omega_{\mathrm{GW}}h^2 \sim 5 \times 10^{-17}$ that is below LISA sensitivity [7].

The vacuum contribution is ultimately cut off at large frequencies, as those never crossed the horizon.

(ii) The contribution from thermal fluctuations, the second term in eq. (3.48), never switches off completely but it peaks at reheating, when $T\eta$ is maximal. At the same time, this part is suppressed at small frequencies. A simple way to see this is to consider the sub-horizon production rate [43] (now written with co-moving conformal coordinates),

$$\frac{\mathrm{d}e_{\mathrm{GW}}(\tau)}{\mathrm{d}\tau\,\mathrm{d}\ln k} \overset{k/a}{\lessapprox} {}^{\alpha^2 T} \frac{16k^3 GT\eta}{\pi a^2} \,, \tag{4.8}$$

which shows the characteristic $\sim k^3$ shape. The growth implies that it might be possible to satisfy CMB constraints on the tensor-to-scalar ratio r at very small $f_0 \ll 10^{-15}\,\mathrm{Hz}$, yet incorporate a growing thermal part, perhaps approaching the LISA sensitivity window at larger frequencies $f_0 \sim (10^{-4}{-}10^{-1})\,\mathrm{Hz}$.

(iii) At very large frequencies, the growing thermal production is cut off at the scale $k/a \sim \pi T$, corresponding to the microwave frequency range $f_0 \sim 10^{11}\,\mathrm{Hz}$ today [43]. Around this domain, gravitational waves do not originate from hydrodynamic fluctuations as considered in section 3.2, but rather from microscopic particle collisions [22].

In order to determine the thermal contribution to $\mathcal{P}_{\mathrm{T}}$ quantitatively, we return to eq. (3.48). Given that the thermal contribution originates at a late stage, when $T\eta$ peaks, the Hubble rate is no longer constant (cf. the second panel in figure 3). Therefore we cannot use the de Sitter spacetime Green's function from eq. (3.26). But an approximate solution

JCAP12(2022)020

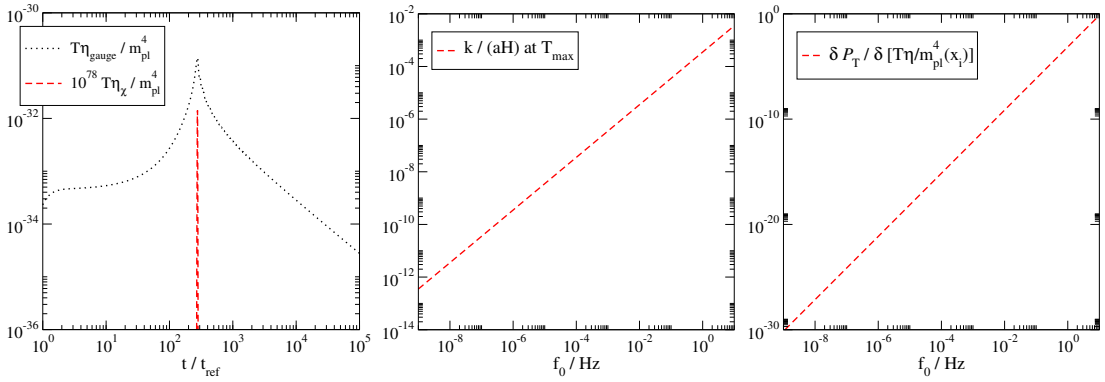

Figure 5. The ingredients influencing the thermal contribution to eq. (3.48) for the benchmark solution in figure 3. Left: source terms for thermal fluctuations, namely temperature times the shear viscosity normalized to $m_{\rm pl}^4$, from eqs. (3.42) and (3.43). Middle: the co-moving physical momentum k/a compared with the Hubble rate at the time when $T\eta$ peaks, i.e. $t \approx 276 t_{\rm ref}$. Right: the (universal) transfer function between $T\eta$ and the gravitational power spectrum at the end of inflation, cf. eq. (4.9), with the time t_i chosen to coincide with the moment when $T\eta$ peaks.

can still be found, making use of the fact that the relevant modes are well outside of the horizon when the maximal $T\eta$ is reached (cf. the middle panel in figure 5).[15]

Making use of the logarithmic time variable x introduced in eq. (2.6), we can write the differential contribution to eq. (3.48) as

$$\frac{\delta \mathcal{P}_{\rm T}(k)}{\delta G^2 T\eta(x_i)} = 32^2\, k^3\, G_{\rm R}^2(\tau_e, \tau_i, k)\, \underbrace{\frac{t_i}{a(t_i)}}_{\partial\tau_i/\partial x_i} \,. \tag{4.9}$$

All quantities appearing here (k^3, $G_{\rm R}^2$, $t_i/a(t_i)$) are dimensionless. Imposing the initial conditions from eq. (3.25) and omitting k^2 from eq. (3.44) as we are looking at modes with $k \ll aH$, the Green's function can be solved for, with the result

$$G_{\rm R}(\tau_e, \tau_i, k) \overset{k\ll aH}{\approx} a^2(\tau_i) \int_{\tau_i}^{\tau_e} \frac{{\rm d}\tau}{a^2(\tau)} = a^2(t_i) \int_{t_i}^{t_e} \frac{{\rm d}t}{a^3(t)} \,. \tag{4.10}$$

This is independent of k, and therefore $G_{\rm R}$ is non-singular at small momenta.

Combining eqs. (4.9) and (4.10), we establish the scaling k^3 of the thermal contribution to $\mathcal{P}_{\rm T}(k)$ for super-horizon modes. Previously, eq. (4.8) had shown this for sub-horizon modes, i.e. with $H \ll k/a \ll \pi T$. As the co-moving momentum k is proportional to the current-day frequency f_0, the scaling is $\sim f_0^3$ in terms of the latter variable. The exact numerical solution is shown in the right-most panel in figure 5, and reproduces this power-law. Afterwards, the spectral shape is modified by the transfer function, cf. figure 1 (right), but in the LISA frequency window the modification of the shape is insignificant (for the amplitude it is $\approx 10^{-6}$).

We stress that the frequency shape $\sim f_0^3$ is universal, whereas its numerical coefficient is model dependent. The model dependence enters through the value of the shear viscosity. In our benchmark solution, where the temperature is small compared with the inflaton

[15] It may be wondered whether it is consistent to apply thermal arguments to modes outside of the horizon. We do this with the logic that a brief moment earlier the modes were still within the horizon, and their fluctuation spectrum was determined by the corresponding dynamics.

JCAP12(2022)020

n	$\partial_c\{V(\pi f_b)\}_{c=0}$	$\partial_c\{\lvert V_{\varphi\varphi}(\pi f_b)\rvert\}_{c=0}$	$\partial_c\{1-n_s\}_{c=0}$	$\partial_c\{r\}_{c=0}$	$\partial_c\{T_{\rm max}/m_{\rm pl}\}_{c=0}$
2	< 0	< 0	-0.011	-0.035	-1.6×10^{-11}
3	< 0	$= 0$	-0.021	$+0.041$	-3.9×10^{-11}

Table 1. Changes resulting from the potential in eq. (4.12), compared with the case $n = 1$ from eq. (1.2). The derivatives have been evaluated at our benchmark point $f_b = 1.25\,m_{\rm pl}$, $m = 1.09\times10^{-6}\,m_{\rm pl}$ and $g_* = 17$, keeping the number of e-folds before $T_{\rm max}$ fixed at $\Delta N = 60$. The case $n = 2$, $c > 0$, which flattens the potential at top, brings down both $1-n_s$ and r, which is preferable for phenomenology (cf. figure 2 (middle)). However, $T_{\rm max}$ hardly changes, and then in the negative direction.

mass, $T \ll m$, the shear viscosity originating from interactions between the inflaton and the radiation bath, eq. (3.42), is exponentially small,

$$T\eta_\chi \overset{T\ll m}{\approx} \frac{T^5}{\Upsilon}\left(\frac{m}{2\pi T}\right)^{3/2}\exp\left(-\frac{m}{T}\right) . \tag{4.11}$$

The dominant contribution originates from the gauge sector, as given by eq. (3.43). Both contributions are illustrated in the left panel of figure 5. Multiplying the left and right panels of figure 5 together with the post-inflationary transfer function from figure 1 (right), the contribution is much below the observable level.

We end by noting that the insignificance of thermal contributions for our benchmark solution can be inferred also from considering the second panel of figure 3. It shows that $T \ll H$ during inflation and around the time when $T\eta$ peaks. This implies that thermal effects are sub-dominant (cf. the discussion in the second paragraph of section 2). In contrast, scenarios leading to $\alpha^2 T \gtrsim H$, which could be self-consistently treated with our formalism [21], might lead to a more substantial signal.

4.3 Other forms of the inflaton potential

As explained at the end of the previous section, our benchmark potential, eq. (1.2), only leads to small thermal effects for the parameter values that are close to being phenomenologically acceptable. We would now like to probe small modifications to the shape of the potential. Inspired by ref. [53], we do this in the minimal manner of a small contribution from higher harmonics. With the constraints $V(j\,2\pi f_b) = V_\varphi(j\,2\pi f_b) = 0$ and $V_{\varphi\varphi}(j\,2\pi f_b) = m^2$, where $j \in \mathbb{Z}$, such a change can be parametrized as

$$V(\bar\varphi) \simeq m^2 f_b^2\left\{(1-c)\left[1-\cos\left(\frac{\bar\varphi}{f_b}\right)\right] + \frac{c}{n^2}\left[1-\cos\left(\frac{n\bar\varphi}{f_b}\right)\right]\right\} . \tag{4.12}$$

The basic characteristics of such potentials, for $n = 2, 3$ and allowing for both signs of c, are listed in table 1. We have again treated thermal effects both by a direct change $m^2 \to m_T^2$, and by the minimal recipe of eq. (2.16), finding effectively the same results.

The upshot from table 1 is that our baseline results, as displayed in figure 2, can be brought into $\leq 1\sigma$ agreement with observational constraints, through a minor $n = 2$ adjustment of the shape of the potential. However, this does not bring about larger thermal effects; for this, a more substantial modification of the shape of the potential is needed. Alternatively, a larger $T_{\rm max}$ could be obtained with a smaller g_* (cf. figure 2 (right)), or by considering a plasma in a confined phase (cf. discussion between eqs. (2.3) and (2.4)).

JCAP12(2022)020

5 Conclusions

Non-Abelian gauge fields are believed to thermalize rapidly, rendering warm inflation scenarios generically plausible [19]. In view of this fact, we have considered the contribution of thermal fluctuations to the gravitational wave background that originates during inflation, concentrating specifically on the LISA frequency window. We have derived an interpolating formula, eq. (3.48), which includes both vacuum and thermal contributions, and is not restricted to de Sitter spacetime, which ceases to be a good approximation towards the end of inflation. In section 4.2, we have shown how the thermal part can be evaluated numerically, and how its main features can be understood analytically.

Our key finding is that, in stark contrast to the approximately constant vacuum contribution, the thermal contribution scales as k^3 in terms of the co-moving momentum, or as f_0^3 in terms of the current-day gravitational wave frequency, cf. eq. (4.9). Since the tensor-to-scalar ratio, r, originates from very small frequencies, $f_0 \ll 10^{-15}\,\text{Hz}$, such a growth implies that CMB constraints can be respected, yet the signal could in principle be observable in the LISA window, $f_0 \sim (10^{-4}\text{–}10^{-1})\,\text{Hz}$. The growth is cut off only at very large frequencies, $f_0 \sim 10^{11}\,\text{Hz}$, where most of the gravitational energy density lies [43].

Whether the thermal part could be observable by LISA depends on the coefficient of the f_0^3 growth. The coefficient is proportional to the maximal shear viscosity of the inflaton plus radiation system. We have illustrated this coefficient for a particular model, with an SU(3) plasma coupled to an axion-like inflaton (cf. figure 5 (left)). For the parameter values that satisfy CMB constraints, the effect is way too small to be observable. However, the situation could be different in other models. In particular, those realizing the "strong regime" of warm inflation, can have a higher maximal temperature, and it is sustained for a longer time.

It might be worried that if we increase the coefficient of f_0^3, then we are also likely to put more energy into the high-f_0 end of the gravitational wave spectrum, and may ultimately face a conflict with N_{eff}, which parametrizes the overall energy density (cf. footnote 3). This consideration is similar in spirit to that constraining Abelian axion-like models [14]. We note that the maximal temperature could be increased to $T_{\text{max}} \approx 2 \times 10^{17}\,\text{GeV}$ without any concern [22, 54], which is $\sim 10^7$ higher than in our benchmark solution. Since the coefficient of f_0^3 scales as T^4 (cf. eq. (3.43)), the gravitational wave background in the LISA window would be increased by a factor $\sim 10^{28}$. In view of figure 5, this could bring us close to the observation threshold around the upper end of the LISA window, particularly if the peak in $T\eta$ is broad. Were such models to be found, a quantitative study both of N_{eff} and of the coefficient of f_0^3 would be well merited. Obviously, like in figure 5 of ref. [52], the observational prospects are much brighter for further experimental concepts, like DECIGO.

To summarize, axion-like inflation has been used as a motivation for the LISA physics program, asserting that an observable signal could be obtained in certain Abelian cases [15]. Our study demonstrates that this statement depends on model details, and is unlikely to apply to generic non-Abelian constructions. That said, we also find a model-independent feature in the spectrum, namely a characteristic f_0^3 shape in the LISA frequency window. The coefficient of this component would allow to measure the maximal shear viscosity of the early universe. The existence of such a feature underlines the versatility of the physics information that is contained in the primordial gravitational wave background.

JCAP12(2022)020

Acknowledgments

We thank Saarik Kalia, Germano Nardini and Arttu Rajantie for helpful discussions. This work was partly supported by the Swiss National Science Foundation (SNSF) under grant 200020B-188712.

A On dispersion theory for the medium response

Complementing section 2.3, we recall here the analyticity (Kramers-Kronig) relations governing the real and imaginary parts of the retarded correlator. Let us assume first that all integrals converge. The correlator $C_{\rm R}$ is analytic in the upper half-plane, from which it follows that

$$C_{\rm R}(\omega+i0^+) = \int_{-\infty}^{\infty} \frac{{\rm d}\omega'}{\pi} \frac{\rho(\omega')}{\omega'-\omega-i0^+} \,, \tag{A.1}$$

where $\rho(\omega) \equiv {\rm Im}\, C_{\rm R}(\omega+i0^+)$ is the spectral function. If ρ is known, ${\rm Re}\, C_{\rm R}$ can be determined along the real axis, by taking the real part of eq. (A.1). Often (particularly in vacuum computations), the relation is re-expressed by making use of antisymmetry, $\rho(-\omega) = -\rho(\omega)$, and by introducing the variable $s \equiv \omega^2$. Then

$${\rm Re}\, C_{\rm R}(\sqrt{s}) = \int_0^{\infty} \frac{{\rm d}s'}{\pi}\, \mathbb{P}\, \frac{\rho(\sqrt{s'})}{s'-s} \,, \tag{A.2}$$

where $\mathbb{P}$ denotes the principal value.

An immediate problem is that if ρ does not decrease at large values of the argument, the integral in eq. (A.2) does not converge. In principle the UV side can be ameliorated by carrying out a subtraction on both sides. For instance, if $\rho(s)$ grows less rapidly than $\sim s$, as is typical for cross sections, then

$$\frac{{\rm Re}[C_{\rm R}(\sqrt{s}) - C_{\rm R}(0)]}{s} = \int_0^{\infty} \frac{{\rm d}s'}{\pi}\, \mathbb{P}\, \frac{\rho(\sqrt{s'})}{s'(s'-s)} \,. \tag{A.3}$$

In our case, $\rho(\sqrt{s})$ grows as $s^2/\ln^2(s)$ [35], so a further subtraction would be necessary. Formally we could write

$$\frac{{\rm Re}[C_{\rm R}(\sqrt{s}) - (1+s\partial_s)C_{\rm R}(0)]}{s^2} = \int_0^{\infty} \frac{{\rm d}s'}{\pi}\, \mathbb{P}\, \frac{\rho(\sqrt{s'})}{(s')^2(s'-s)} \,, \tag{A.4}$$

however now the problem has been transferred to the IR side. Indeed, at finite temperature, spectral weight decreases only slowly at small frequency, $\rho(\sqrt{s'}) \sim \sqrt{s'}$, so the integral in eq. (A.4) does not converge at small s'. Therefore one should rather make use of eq. (A.3), and regularize the UV part.

Let us recall another aspect associated with the subtractions. Suppose that we add a real polynomial, say $a_0 + a_1 s + a_2 s^2 + \ldots$, to $C_{\rm R}$. This is analytic in the upper half-plane, and thus in principle a viable addition. It gives no contribution to ${\rm Im}\, C_{\rm R}$ along the real axis, i.e. to $\rho(\sqrt{s})$, simply because there is no imaginary part. But it would still appear on the left-hand side of eqs. (A.2)–(A.4). This underlines the fact that dispersion relations are meaningful only via a careful handling of subtractions.

JCAP12(2022)020

Now, let us illustrate the situation by assuming that the spectral function has a Lorentzian shape at small frequencies [21],

$$\rho(\omega) \simeq \rho_{\text{IR}}(\omega) \equiv \frac{\omega\Delta^2\Upsilon_{\text{IR}}}{\omega^2+\Delta^2} \,. \tag{A.5}$$

Then the integrals in eqs. (A.1) and (A.2) converge. Carrying them out yields

$$\text{Re}\, C_{\text{R,IR}}(\omega) = \frac{\Delta^3\Upsilon_{\text{IR}}}{\omega^2+\Delta^2} = \Delta\Upsilon_{\text{IR}}\left\{1-\frac{\omega^2}{\omega^2+\Delta^2}\right\} . \tag{A.6}$$

In contrast, the subtracted relation in eq. (A.3) only gives information on the ω-dependent part (the second term in eq. (A.6)). At the same time, $C_{\text{R}}(0)$ for the operator χ from eq. (1.1) vanishes in perturbation theory. It is for this reason that the constant part of eq. (A.6) was cancelled by the addition of $a_0 \equiv -\Delta\Upsilon_{\text{IR}}$ in ref. [21]. However, the consistency of this procedure is unclear, because the growing vacuum part of ρ was omitted. Because of these complications, it is more straightforward to compute $\text{Re}\, C_{\text{R}}$ directly, as we did in section 2.3.

References

[1] A.A. Starobinsky, *Spectrum of relict gravitational radiation and the early state of the universe*, *JETP Lett.* **30** (1979) 682 [INSPIRE].

[2] Planck collaboration, *Planck 2018 results. X. Constraints on inflation*, *Astron. Astrophys.* **641** (2020) A10 [arXiv:1807.06211] [INSPIRE].

[3] S.Y. Khlebnikov and I.I. Tkachev, *Relic gravitational waves produced after preheating*, *Phys. Rev. D* **56** (1997) 653 [hep-ph/9701423] [INSPIRE].

[4] R. Easther and E.A. Lim, *Stochastic gravitational wave production after inflation*, *JCAP* **04** (2006) 010 [astro-ph/0601617] [INSPIRE].

[5] J. García-Bellido, D.G. Figueroa and A. Sastre, *Gravitational wave background from reheating after hybrid inflation*, *Phys. Rev. D* **77** (2008) 043517 [arXiv:0707.0839] [INSPIRE].

[6] J.-F. Dufaux, G. Felder, L. Kofman and O. Navros, *Gravity waves from tachyonic preheating after hybrid inflation*, *JCAP* **03** (2009) 001 [arXiv:0812.2917] [INSPIRE].

[7] R. Flauger, N. Karnesis, G. Nardini, M. Pieroni, A. Ricciardone and J. Torrado, *Improved reconstruction of a stochastic gravitational wave background with LISA*, *JCAP* **01** (2021) 059 [arXiv:2009.11845] [INSPIRE].

[8] K. Freese, J.A. Frieman and A.V. Olinto, *Natural inflation with pseudo Nambu-Goldstone bosons*, *Phys. Rev. Lett.* **65** (1990) 3233 [INSPIRE].

[9] M.M. Anber and L. Sorbo, *Naturally inflating on steep potentials through electromagnetic dissipation*, *Phys. Rev. D* **81** (2010) 043534 [arXiv:0908.4089] [INSPIRE].

[10] E. Pajer and M. Peloso, *A review of Axion Inflation in the era of Planck*, *Class. Quant. Grav.* **30** (2013) 214002 [arXiv:1305.3557] [INSPIRE].

[11] J.L. Cook and L. Sorbo, *Particle production during inflation and gravitational waves detectable by ground-based interferometers*, *Phys. Rev. D* **85** (2012) 023534 [*Erratum ibid.* **86** (2012) 069901] [arXiv:1109.0022] [INSPIRE].

[12] N. Barnaby, E. Pajer and M. Peloso, *Gauge field production in axion inflation: consequences for monodromy, non-Gaussianity in the CMB, and gravitational waves at interferometers*, *Phys. Rev. D* **85** (2012) 023525 [arXiv:1110.3327] [INSPIRE].

JCAP12(2022)020

[13] M.M. Anber and L. Sorbo, *Non-Gaussianities and chiral gravitational waves in natural steep inflation*, *Phys. Rev. D* **85** (2012) 123537 [arXiv:1203.5849] [INSPIRE].

[14] P. Adshead, J.T. Giblin, Jr., M. Pieroni and Z.J. Weiner, *Constraining axion inflation with gravitational waves from preheating*, *Phys. Rev. D* **101** (2020) 083534 [arXiv:1909.12842] [INSPIRE].

[15] N. Bartolo et al., *Science with the space-based interferometer LISA. IV: Probing inflation with gravitational waves*, *JCAP* **12** (2016) 026 [arXiv:1610.06481] [INSPIRE].

[16] V. Domcke, V. Guidetti, Y. Welling and A. Westphal, *Resonant backreaction in axion inflation*, *JCAP* **09** (2020) 009 [arXiv:2002.02952] [INSPIRE].

[17] A. Caravano, E. Komatsu, K.D. Lozanov and J. Weller, *Lattice Simulations of Axion-*U(1) *Inflation*, arXiv:2204.12874 [INSPIRE].

[18] V. Domcke, Y. Ema and K. Mukaida, *Axion assisted Schwinger effect*, *JHEP* **05** (2021) 001 [arXiv:2101.05192] [INSPIRE].

[19] W. DeRocco, P.W. Graham and S. Kalia, *Warming up cold inflation*, *JCAP* **11** (2021) 011 [arXiv:2107.07517] [INSPIRE].

[20] J. Yokoyama and A.D. Linde, *Is warm inflation possible?*, *Phys. Rev. D* **60** (1999) 083509 [hep-ph/9809409] [INSPIRE].

[21] M. Laine and S. Procacci, *Minimal warm inflation with complete medium response*, *JCAP* **06** (2021) 031 [arXiv:2102.09913] [INSPIRE].

[22] P. Klose, M. Laine and S. Procacci, *Gravitational wave background from non-Abelian reheating after axion-like inflation*, *JCAP* **05** (2022) 021 [arXiv:2201.02317] [INSPIRE].

[23] A. Berera, *Warm inflation*, *Phys. Rev. Lett.* **75** (1995) 3218 [astro-ph/9509049] [INSPIRE].

[24] M. Bastero-Gil, A. Berera, R.O. Ramos and J.G. Rosa, *Warm Little Inflaton*, *Phys. Rev. Lett.* **117** (2016) 151301 [arXiv:1604.08838] [INSPIRE].

[25] K.V. Berghaus, P.W. Graham and D.E. Kaplan, *Minimal warm inflation*, *JCAP* **03** (2020) 034 [arXiv:1910.07525] [INSPIRE].

[26] S. Das, G. Goswami and C. Krishnan, *Swampland, axions, and minimal warm inflation*, *Phys. Rev. D* **101** (2020) 103529 [arXiv:1911.00323] [INSPIRE].

[27] Y. Reyimuaji and X. Zhang, *Warm-assisted natural inflation*, *JCAP* **04** (2021) 077 [arXiv:2012.07329] [INSPIRE].

[28] F. Takahashi and W. Yin, *Challenges for heavy QCD axion inflation*, *JCAP* **10** (2021) 057 [arXiv:2105.10493] [INSPIRE].

[29] V. Kamali, H. Moshafi and S. Ebrahimi, *Minimal warm inflation and TCC*, arXiv:2111.11436 [INSPIRE].

[30] M. Mirbabayi and A. Gruzinov, *Shapes of non-Gaussianity in warm inflation*, arXiv:2205.13227 [INSPIRE].

[31] G. Jackson and M. Laine, *Hydrodynamic fluctuations from a weakly coupled scalar field*, *Eur. Phys. J. C* **78** (2018) 304 [arXiv:1803.01871] [INSPIRE].

[32] G.D. Moore and M. Tassler, *The sphaleron rate in* SU(N) *gauge theory*, *JHEP* **02** (2011) 105 [arXiv:1011.1167] [INSPIRE].

[33] M. Laine, L. Niemi, S. Procacci and K. Rummukainen, *Shape of the hot topological charge density spectral function*, *JHEP* **11** (2022) 126 [arXiv:2209.13804] [INSPIRE].

[34] M. Laine, A. Vuorinen and Y. Zhu, *Next-to-leading order thermal spectral functions in the perturbative domain*, *JHEP* **09** (2011) 084 [arXiv:1108.1259] [INSPIRE].

JCAP12(2022)020

[35] M. Laine, M. Vepsäläinen and A. Vuorinen, *Ultraviolet asymptotics of scalar and pseudoscalar correlators in hot Yang-Mills theory*, *JHEP* **10** (2010) 010 [arXiv:1008.3263] [INSPIRE].

[36] A.A. Starobinsky and J. Yokoyama, *Equilibrium state of a self-interacting scalar field in the de Sitter background*, *Phys. Rev. D* **50** (1994) 6357 [astro-ph/9407016] [INSPIRE].

[37] P. Auclair and C. Ringeval, *Slow-roll inflation at N3LO*, *Phys. Rev. D* **106** (2022) 063512 [arXiv:2205.12608] [INSPIRE].

[38] R.O. Ramos and L.A. da Silva, *Power spectrum for inflation models with quantum and thermal noises*, *JCAP* **03** (2013) 032 [arXiv:1302.3544] [INSPIRE].

[39] E.M. Lifshitz and L.P. Pitaevskii, *Statistical Physics. Part 2*, Butterworth-Heinemann, Oxford, U.K. (1980), sections 88–89.

[40] J.I. Kapusta, B. Müller and M. Stephanov, *Relativistic theory of hydrodynamic fluctuations with applications to heavy-ion collisions*, *Phys. Rev. C* **85** (2012) 054906 [arXiv:1112.6405] [INSPIRE].

[41] P.B. Arnold, G.D. Moore and L.G. Yaffe, *Transport coefficients in high temperature gauge theories. 2. Beyond leading log*, *JHEP* **05** (2003) 051 [hep-ph/0302165] [INSPIRE].

[42] Y. Qiu and L. Sorbo, *Spectrum of tensor perturbations in warm inflation*, *Phys. Rev. D* **104** (2021) 083542 [arXiv:2107.09754] [INSPIRE].

[43] J. Ghiglieri and M. Laine, *Gravitational wave background from Standard Model physics: qualitative features*, *JCAP* **07** (2015) 022 [arXiv:1504.02569] [INSPIRE].

[44] Y. Watanabe and E. Komatsu, *Improved calculation of the primordial gravitational wave spectrum in the standard model*, *Phys. Rev. D* **73** (2006) 123515 [astro-ph/0604176] [INSPIRE].

[45] K. Saikawa and S. Shirai, *Primordial gravitational waves, precisely: the role of thermodynamics in the Standard Model*, *JCAP* **05** (2018) 035 [arXiv:1803.01038] [INSPIRE].

[46] D.J. Schwarz, *Evolution of gravitational waves through cosmological transitions*, *Mod. Phys. Lett. A* **13** (1998) 2771 [gr-qc/9709027] [INSPIRE].

[47] S. Weinberg, *Damping of tensor modes in cosmology*, *Phys. Rev. D* **69** (2004) 023503 [astro-ph/0306304] [INSPIRE].

[48] http://www.laine.itp.unibe.ch/eos15/.

[49] M. Laine and Y. Schröder, *Quark mass thresholds in QCD thermodynamics*, *Phys. Rev. D* **73** (2006) 085009 [hep-ph/0603048] [INSPIRE].

[50] M. Laine and M. Meyer, *Standard Model thermodynamics across the electroweak crossover*, *JCAP* **07** (2015) 035 [arXiv:1503.04935] [INSPIRE].

[51] A. Ringwald, K. Saikawa and C. Tamarit, *Primordial gravitational waves in a minimal model of particle physics and cosmology*, *JCAP* **02** (2021) 046 [arXiv:2009.02050] [INSPIRE].

[52] A. Ringwald and C. Tamarit, *Revealing the cosmic history with gravitational waves*, *Phys. Rev. D* **106** (2022) 063027 [arXiv:2203.00621] [INSPIRE].

[53] R. Daido, F. Takahashi and W. Yin, *The ALP miracle: unified inflaton and dark matter*, *JCAP* **05** (2017) 044 [arXiv:1702.03284] [INSPIRE].

[54] J. Ghiglieri, G. Jackson, M. Laine and Y. Zhu, *Gravitational wave background from Standard Model physics: Complete leading order*, *JHEP* **07** (2020) 092 [arXiv:2004.11392] [INSPIRE].

JCAP12(2022)020